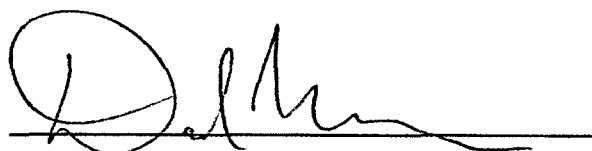


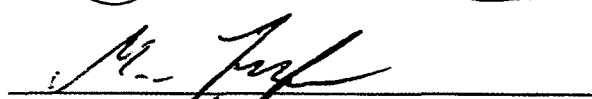
SIZE EFFECTS IN MESOSCALE MECHANICAL TESTING OF SNOW

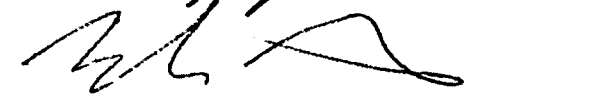
By

Daisy Huang

RECOMMENDED:



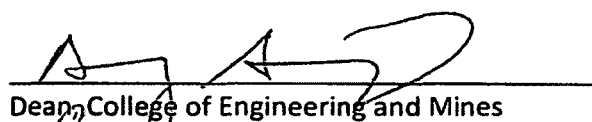


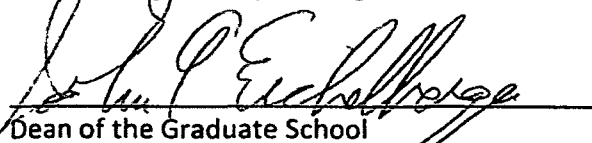


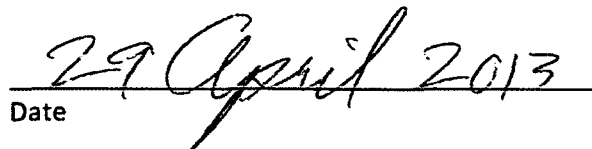
  
Advisory Committee Chair

  
Chair, Department of Mechanical Engineering

APPROVED:

  
Dean, College of Engineering and Mines

  
Dean of the Graduate School

  
Date



SIZE EFFECTS IN MESOSCALE MECHANICAL TESTING OF SNOW

A

DISSERTATION

Presented to the Faculty

of the University of Alaska Fairbanks

in Partial Fulfillment of the Requirements

for the Degree of

DOCTOR OF PHILOSOPHY

By

Daisy Huang, M.S., B.S.

Fairbanks, Alaska

May 2013

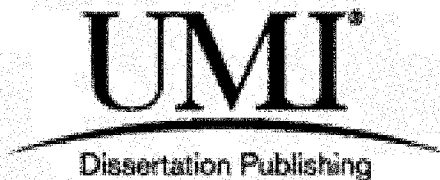
UMI Number: 3573015

All rights reserved

INFORMATION TO ALL USERS

The quality of this reproduction is dependent upon the quality of the copy submitted.

In the unlikely event that the author did not send a complete manuscript and there are missing pages, these will be noted. Also, if material had to be removed, a note will indicate the deletion.



UMI 3573015

Published by ProQuest LLC 2013. Copyright in the Dissertation held by the Author.

Microform Edition © ProQuest LLC.

All rights reserved. This work is protected against unauthorized copying under Title 17, United States Code.



ProQuest LLC  
789 East Eisenhower Parkway  
P.O. Box 1346  
Ann Arbor, MI 48106-1346

**Abstract**

Snow is a naturally-occurring, heterogeneous material whose interactions with humans make it desirable for analysis as a geotechnical engineering material. In this study, clean, undisturbed, natural snows of two common types were collected in and around Fairbanks, Alaska and subjected to laboratory testing, and the results were compiled and analyzed. Three types of tests—flat pin indentation, unconfined compression, and cone penetration—were carried out while varying size parameters, and size effects were observed and studied. From flat-pin indentation testing, it was observed that first peak indentation strength initially fell exponentially with increasing indenter cross-sectional area, with the exponent averaging 0.84. Furthermore, the strength eventually rose to a plateau value, and the compression strength of snow could be calculated from this plateau value. This plateau, too, initially depended exponentially on the pin cross-sectional area for smaller pins. From unconfined compression testing, it was observed that as cross-sectional area of a flat pin indenter increased, plateau strength eventually reached that value found from unconfined compression testing. Furthermore, initial strength, plateau strength, and energy absorption density all increased linearly with increasing aspect ratio. From cone penetration testing, it was found that empirical values of snow strength may be obtained on both a micromechanical and macromechanical scale using cone penetration. Size effects, were also observed—smaller cone diameters and larger cone included angles yielded larger values for apparent snow strength. Some of the mechanisms behind all of these size effects are explainable from theory; others must be regarded for now as empirical in nature. In both cases, the results are quite reliable descriptors for a natural material, and may be safely interpolated from.

## Table of Contents

	<b>Page</b>
<b>Signature Page</b> .....	<b>i</b>
<b>Title Page</b> .....	<b>ii</b>
<b>Abstract</b> .....	<b>iii</b>
<b>Table of Contents</b> .....	<b>iv</b>
<b>List of Figures</b> .....	<b>ix</b>
<b>List of Tables</b> .....	<b>xii</b>
<b>Preface and Background</b> .....	<b>xiii</b>
<b>1 Introduction</b> .....	<b>1</b>
<b>1.1 Selection and description of snows</b> .....	<b>4</b>
<b>1.2 Comparison among the three types of tests</b> .....	<b>5</b>
<b>1.3 Overview</b> .....	<b>5</b>
<b>2 Mechanical properties of snow using indentation tests: size effects</b> .....	<b>7</b>
<b>2.1 Introduction</b> .....	<b>7</b>
<b>2.2 Background</b> .....	<b>9</b>
2.2.1 Earlier work.....	9
2.2.2 Indentation model .....	12
2.2.3 Plateau strength analysis of foams.....	13
<b>2.3 Experimental procedures</b> .....	<b>14</b>
2.3.1 Collection and storage of snow .....	14
2.3.2 Snow characterization .....	15

	<b>Page</b>
2.3.3 Establishment of testing parameters.....	16
2.3.3.1 Selection of Snows .....	16
2.3.3.2 Pin Selection.....	17
2.3.3.3 Confirmation of Indentation Model Using CT Scans.....	18
2.3.3.4 Initial Sensitivity Studies .....	20
2.3.4 Tribometer setup.....	22
2.3.5 Test parameters.....	23
<b>2.4 Results.....</b>	<b>25</b>
2.4.1 Stress-displacement curves .....	25
2.4.2 First peak strength.....	28
2.4.3 Plateau strength (zone II).....	31
2.4.4 Absorption of energy .....	35
<b>2.5 Discussion.....</b>	<b>38</b>
2.5.1 First peak strength.....	38
2.5.2 Plateau strength.....	39
2.5.3 Energy absorption.....	40
<b>2.6 Conclusions.....</b>	<b>41</b>
<b>Acknowledgements.....</b>	<b>43</b>
<b>References.....</b>	<b>44</b>
<b>3 Mechanical properties of snow using compression tests: size effects .....</b>	<b>48</b>
<b>3.1 Introduction.....</b>	<b>48</b>

	Page
<b>3.2 Experimental procedures .....</b>	<b>50</b>
3.2.1 Selection, collection, and storage of snow .....	51
3.2.2 Instron setup for unconfined compression testing .....	51
3.2.3 Test parameters .....	52
<b>3.3 Results .....</b>	<b>53</b>
3.3.1 Characterization of snows .....	53
3.3.2 Failure modes .....	54
3.3.3 Pressure-displacement curves .....	56
3.3.4 First peak strength .....	58
3.3.5 Plateau strength .....	59
3.3.6 Absorption of energy .....	61
<b>3.4 Discussion .....</b>	<b>63</b>
3.4.1 Overall test observations .....	63
3.4.2 Discussion of results .....	65
<b>3.5 Conclusions .....</b>	<b>66</b>
<b>Acknowledgements .....</b>	<b>67</b>
<b>References .....</b>	<b>69</b>
<b>4 Mechanical properties of snow using cone penetration tests: size effects .....</b>	<b>71</b>
<b>4.1 Introduction .....</b>	<b>72</b>
<b>4.2 Background .....</b>	<b>73</b>
4.2.1 Prior work .....	73



4.2.2	Cone penetration theory .....	75
<b>4.3</b>	<b>Experimental procedures .....</b>	<b>76</b>
4.3.1	In-situ snow testing, collection, and characterization .....	77
4.3.1.1	Snow MicroPenetrometer.....	78
4.3.1.2	Other on-site snow characterization tests.....	81
4.3.1.3	Collection and storage of snow.....	81
4.3.1.4	Laboratory testing of snow for confirmation of snow selection.....	82
4.3.2	Cone penetration testing.....	83
4.3.2.1	Test parameters .....	84
<b>4.4</b>	<b>Results.....</b>	<b>85</b>
4.4.1	Characterization of snows .....	85
4.4.1.1	Characterization of snows from SMP.....	86
4.4.1.2	Characterization of snows via visual examination .....	87
4.4.2	Laboratory cone penetration results.....	88
4.4.2.1	Effects of snow grain size.....	90
4.4.2.2	Effects of varying cone angle .....	91
4.4.2.3	Effects of varying cone diameter in laboratory cone penetration.....	93
<b>4.5</b>	<b>Discussion.....</b>	<b>95</b>
<b>4.6</b>	<b>Conclusions.....</b>	<b>96</b>
	<b>Acknowledgements.....</b>	<b>97</b>
	<b>References.....</b>	<b>98</b>

**Page**

<b>5</b>	<b>Discussion and limitations.....</b>	<b>101</b>
<b>6</b>	<b>Conclusions .....</b>	<b>102</b>
<b>7</b>	<b>Additional publications by the author .....</b>	<b>104</b>

## List of Figures

	Page
<b>Fig. 1.</b> Accumulation of pressure bulb under a flat indenter pin .....	3
<b>Fig. 2.</b> Theoretical stress/displacement relationship for indentation into snow. ....	12
<b>Fig. 3.</b> Size effects of different indenter geometries.....	17
<b>Fig. 4.</b> CT scans of indented snow (white is ice).....	18
<b>Fig. 5.</b> Cross sections of CT scan of indented snow, 12.7 mm indenter (white is ice).....	19
<b>Fig. 6.</b> Cross sections of CT scan of indented snow, 6.35 mm indenter (white is ice).....	19
<b>Fig. 7.</b> Indentation test setup. ....	23
<b>Fig. 8.</b> Stress-displacement curves for 12.7 mm pin indentations into fine snow. ....	26
<b>Fig. 9.</b> Stress-displacement curves comparing pin sizes and snow types. ....	27
<b>Fig. 10.</b> Stress-displacement curves for 12.7 mm pin indentations, comparing two snow types.	28
<b>Fig. 11.</b> Example of first failure strength data, fine-grained snow. ....	29
<b>Fig. 12.</b> Relationship between plateau strength and pin diameter, for (a) fine grained snow and (b) coarse-grained snow (there is only one data point at 12.7 mm). ....	32
<b>Fig. 13.</b> Plateau force / $\pi r$ as a function of pin radius at $2 \text{ mm s}^{-1}$ for (a) fine-grained and (b) coarse-grained snow.....	34
<b>Fig. 14.</b> Energy absorption density during pin indentation into (a) fine-grained and (b) coarse- grained snow.....	37
<b>Fig. 15.</b> Unconfined compression test.....	52
<b>Fig. 16.</b> Unconfined compression of 47dx44h cylinders of sintered snow, stress versus displacement.....	56

<b>Fig. 17.</b> Unconfined compression of 64dx10h cylinders of sintered snow, stress versus displacement.....	57
<b>Fig. 18.</b> First peak strength versus aspect ratio.....	58
<b>Fig. 19.</b> First peak strength versus cross-sectional area.....	59
<b>Fig. 20.</b> Plateau strength versus aspect ratio .....	60
<b>Fig. 21.</b> Plateau strengths of indentation and compression data .....	61
<b>Fig. 22.</b> Energy absorption versus diameter .....	62
<b>Fig. 23.</b> Energy absorption versus aspect ratio .....	63
<b>Fig. 24.</b> First peak strength versus pin area, unsintered snow.....	64
<b>Fig. 25.</b> First peak strength versus pin area, sintered snow .....	65
<b>Fig. 26.</b> SMP in field test environment .....	79
<b>Fig. 27.</b> Example of SMP output for a complete snowpack reading .....	80
<b>Fig. 28.</b> SMP output, zoomed in to area of interest .....	81
<b>Fig. 29.</b> Cold temperature enclosure.....	83
<b>Fig. 30.</b> Schematic of cone penetration test .....	84
<b>Fig. 31.</b> Optical Examination of Fine-Grained Snow .....	87
<b>Fig. 32.</b> Optical Examination of Coarse-Grained Snow.....	88
<b>Fig. 33.</b> Force-depth data for 30-degree, 3.0-mm cone penetration into fine-grained snow .....	90
<b>Fig. 34.</b> Force-depth data for 30-degree, 3.0-mm cone penetration into coarse-grained snow ..	91
<b>Fig. 35.</b> Force-depth data for 15-degree, 3.0-mm cone penetration into fine-grained snow .....	92
<b>Fig. 36.</b> Force-depth data for 45-degree, 3.0-mm cone penetration into fine-grained snow .....	92

	<b>Page</b>
<b>Fig. 37. Macromechanical Strength vs. Cone Angle .....</b>	<b>93</b>
<b>Fig. 38. Force-depth data for 30-degree, 2.5-mm cone penetration into fine-grained snow .....</b>	<b>94</b>
<b>Fig. 39. Force-depth data for 30-degree, 4.0-mm cone penetration into fine-grained snow .....</b>	<b>94</b>
<b>Fig. 40. Macromechanical Strength vs. Diameter Squared .....</b>	<b>95</b>

**List of Tables**

	<b>Page</b>
<b>Table 1.</b> Indentation test parameters.....	24
<b>Table 2.</b> Exponent from a range of tests.....	30
<b>Table 3.</b> Mean plateau strengths from a range of tests. ....	31
<b>Table 4.</b> Compaction and shear terms from a range of tests. ....	35
<b>Table 5.</b> Unconfined compression testing parameters.....	53
<b>Table 6.</b> Failure modes of different aspect ratios.....	55
<b>Table 7.</b> Test parameters .....	85
<b>Table 8.</b> SMP In situ results.....	86
<b>Table 9.</b> Snow penetration test results.....	89

## **Preface and Background**

This study was funded by the U.S. Army Tank Automotive Research, Development and Engineering Center (TARDEC), and their interest was in tractive properties of snow with regards to ground vehicle traversal. Because frozen ground under the snow is comparatively of infinite stiffness, the properties of the snow dominate the ground side of the snow-vehicle interface.

The mechanics of a tire or tank tread traversing snow may be analyzed in two parts: First, the indentation as the tire or tread first makes contact and the snow receives the weight; and second, the traversal, which is a combination of plowing and sliding. This study focused on the first part. To be presented here are results and analysis from a series of surface tests of snow.

Not discussed in this dissertation, but also funded and executed under the same study and with results publically available, is a series of vehicle-snow tests that examined ground-tire interactions on a system level. This was achieved using a 3-dimensional laser profilometer in conjunction with an instrumented vehicle with accelerometers mounted on all four tires and a computer that synchronized the accelerometers' output with data from the vehicle's control system. The two vehicles (one with the profilometer, the other with the mechanical measurement system) were used to obtain information about the different forces that occur between tires and snow when a vehicle interacts with snowy terrain. More information about this is available in papers listed in the conclusions chapter.

The author wishes to thank her adviser, Jonah H. Lee; past and current committee members, David Newman, Rorik Peterson, Martin Truffer, and Gang Chen; H.P. Marshall for help

with the Snow MicroPenetrometer; and Martin Scheebeli and Henning Loewe of the Swiss Institute for Snow and Avalanche Research for advice.

We gratefully acknowledge support for this work by the U.S. Army TACOM Life Cycle Command under Contract No. W56HZV-08-C-0236, through a subcontract with Mississippi State University. This work was performed in part for the Simulation Based Reliability and Safety (SimBRS) research program. Any opinions, findings and conclusions or recommendations expressed in this material are those of the authors and do not necessarily reflect the views of the U.S. Army TACOM.

Disclaimer: Reference herein to any specific commercial company, product, process, or service by trade name, trademark, manufacturer, or otherwise, does not necessarily constitute or imply its endorsement, recommendation, or favoring by the United States Government or the Department of the Army (DoA). The opinions of the authors expressed herein do not necessarily state or reflect those of the United States government or the DoA, and shall not be used for advertising or product endorsement purposes.



## 1 Introduction

Mechanical behavior of snow is of interest to biologists and geologists, who are interested in ground cover properties; alpinists, who study avalanches; and engineers, who must design vehicles and sports equipment that traverse snow. Therefore, the history of the study of snow has been broad, and has ranged from scales of interest from the  $10^{-3}$  to the  $10^2$  m range. This study has focused on interactions on mesoscale ranges, which are the smallest scales on which bulk properties may begin to be discerned. The reason for this is that we were interested in examining snow mechanical properties on a level that is as fundamental as possible, but still large enough to (i) obtain behavior of full crystals and not water molecules and (ii) obtain behavior of bulk snow as a terrain material. As engineers, our range of interest is about that of a tire tread, which is on the order of mm to cm.

Other parameters that were established to maintain this study to focus as much as possible on the pertinent fundamental characteristics of snow were:

1. Snows were selected that were metamorphically stable. This is the type that is most commonly encountered by ground vehicles in snowy regions since it, by definition, is the most temporally stable.
2. The testing interfaces (pins, indenters, compression platens, etc.) were selected to be made of materials significantly harder than snow and effectively infinitely stiff in comparison. The purpose of this was so that test results would give the properties of the snow side only, and not of the tester side.

3. Temperatures were selected (by selection of snow collecting days) and/or artificially maintained (in a cold room or a storage freezer) to be significantly below the melting point of water ( $< -20^{\circ}\text{C}$ ). This was so that the effects from the presence of liquid water and water menisci could be minimized.
4. Testing speeds were selected to be well below any that would come close to generating thermal effects during testing.
5. Only natural snows were used in testing. Also the snows were carefully selected to be of a particular common type. Moreover, the snows were carefully collected to be as little disturbed as possible, and no sorting of grains was performed before testing.

In pursuit of the fundamental properties of snow on the mesoscale, various testing methodologies were tried, including:

1. Flat pin indentation
1. Cone penetration
2. Unconfined compression
3. Thin blade indentation
4. Pin on disc tribometer friction testing
5. Pin on disc tribometer plowing testing

Of the different types of testing, flat pin indentation, cone penetration, and unconfined compression yielded the most consistent and interesting results; thus, results from these three sets of testing were selected for publication.

All three of these types of tests were based on vertical deformation in the direction of gravity. All three also showed that an object deforming snow accumulates a pressure bulb

around it, and that the pressure bulb grows, increasing the resisting force, until it reaches a finite size. At this point, the pressure bulb proceeds through the snow along with the testing probe, effectively increasing the volume of its leading edge. This is shown in Fig. 1.

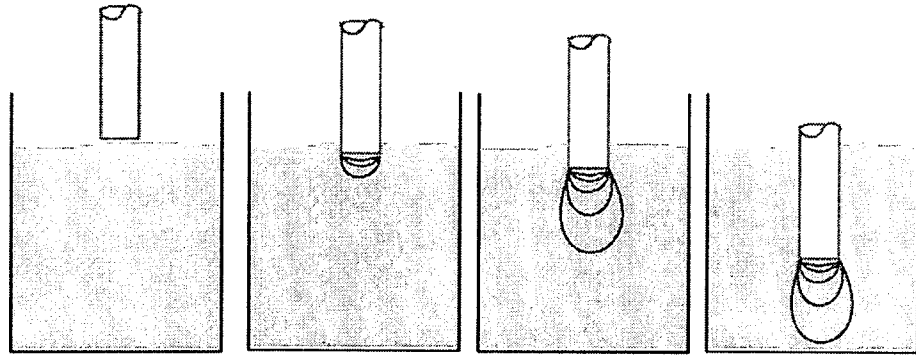


**Fig. 1.** Accumulation of pressure bulb under a flat indenter pin

## 1.1 Selection and description of snows

Snows were desired that were metamorphically stable and commonly found, especially where people live and are likely to need to traverse it. In order to select snow types, many examination techniques were used, including:

- Optical examination *in situ* using a hand magnifier.
- Weighing at the collection sites using graduated cylinders and a spring scale, to obtain density of different snow types.
- Sieving at the collection sites using 4 different-sized grates, to obtain grain size distribution of different snow types.
- Optical examination in a cold room under a light microscope.
- CT 3D X-ray MicroTomography scanning (in a cold room) to obtain three-dimensional structure of different snow types.

The above tools were used, and the selection criteria yielded two types of snow in and around Fairbanks. Both consist of roughly uniformly rounded grains that have had most of their sharper features either eroded or sublimated off.

The first type, which will henceforth be called “fine-grained snow”, has an average grain size of less than 1 mm. This is the type that is found near the surface of nearly all undisturbed snow packs throughout most of winter in the Fairbanks region, in years when there are no anomalous weather events. As long as snow does not see a thaw-freeze cycle, its natural evolution while sitting in a dry, cold, windless environment is toward this type, and it gets there pretty quickly (within a few days to a few weeks after falling).

The second type, which will henceforth be called “coarse-grained snow”, has an average grain size of over 1.5 mm. This is a type that grows when exposed to a thermal gradient, such as while being insulated against a forest ground from below, while being exposed to cold from the atmosphere from above. This type of snow is found under the top few 10s of cm of snow later in winter (starting around February). It is found a bit earlier in winter where thermal gradients are particularly strong, such as over the Tanana River or over a pond that does not fully freeze.

## **1.2 Comparison among the three types of tests**

Commonalities among the three types of tests performed were that in each, the size scales were varied. That means that the pin diameters, the cone penetrator geometries, and the heights and diameters of the snow samples used in unconfined compression testing were all varied. Size effects are commonly observed in other geological materials, so we wished to determine whether snow could be tested and analyzed in an analogous manner to other terrain materials.

## **1.3 Overview**

The following chapters are comprised of three papers. The first, “Mechanical properties of snow using indentation tests: size effects”, has been published in the *Journal of Glaciology*. The second, “Mechanical properties of snow using compression tests: size effects”, has been submitted to the *Journal of Glaciology* as a follow-up to the first. The premise behind coupling these papers is that as the indenter size during an indentation test grows very large, at some point the indentation test becomes effectively a compression test. This relationship is discussed in the compression chapter.

The third paper, “Mechanical Properties of Snow using Cone Penetration Tests: Size Effects”, will be submitted to *Cold Regions Science and Technology*. While maintaining as much as possible parameters to make the penetration tests analogous to the indentation and compression tests, the cone penetration study has borrowed methods and thought processes from the geological sciences. Since cone penetration is a tool commonly used by people analyzing soils as structural materials, the *Cold Regions Science and Technology* was deemed a fitting choice.

## **2 Mechanical properties of snow using indentation tests: size effects<sup>1</sup>**

**ABSTRACT.** An attempt is made to obtain and quantify the mechanical properties of two common types of seasonal snow on the ground. Different samples of natural snow whose metamorphism had stabilized (such as would remain on a road throughout winter in a cold, snowy area) were gathered and tested using mesoscale indentation tests (metrics on the order of mm to cm). Results from the stress vs. displacement curves from indentation indicated that (1) first peak strength decreased, according to a power law, with increasing indenter size and was not affected by snow average grain size, (2) plateau strength decreased with increasing indenter size and snow compaction strength might be calculated from these data, and (3) mean energy absorption density during indentation was independent of indenter size in some size ranges, and decreased with increasing indenter size in other size ranges.

### **2.1 Introduction**

Systematic studies of snow provide useful data to natural scientists who study snow behavior under stresses from forces of nature, and to engineers who study how snow impacts the behavior of vehicles that traverse snow. Thus, quantitative measurement and description of snow mechanical behavior is desirable.

Indentation tests, common in materials science, have been used extensively in vehicle/snow interaction studies to obtain stress-displacement relationships (Jellinek, 1957; Yong and Fukue, 1977; Edens and Brown, 1991; Shoop and Alger, 1998). Snow can be viewed as a porous random heterogeneous material (Yuan and others, 2010), similar to foams (Kirchner

---

<sup>1</sup> Huang, D. and J.H. Lee, Journal of Glaciology, v59, No. 213, 2013

and others, 2001) whose mechanical properties are known to be dependent on the size of the samples (Olurin and others, 2000; Kirchner and others, 2001; Onck and others, 2001; Ramamurty and Kumaran, 2004; Lu and others, 2008). In tire/snow interactions, the tire and its tread are in contact with the snow on varying length scales. The study of the size effect of snow is thus important for both materials science and application.

The mechanical properties of snow depend on microstructure, which is a product of the environment during formation, the thermal and humidity history that the snow has experienced since its formation, and the current environment. In this study, choices were made to narrow the snow types under study using two criteria. The first of these criteria was availability. The second was the usefulness and applicability of results. For the latter criterion, only relatively stable types of snows were selected for study, because a fresh snowfall, by definition, does not remain on the ground for long before it metamorphoses into a more stable snow type. This stable snow is the type most likely to be encountered because it, by definition, remains on the ground in the environment for long periods. In Fairbanks, Alaska, where such quasi-stable snow is available for the duration of long, cold, dry winters, the first criterion above, availability, is also nicely satisfied.

Two common and stable types of snow were selected; test parameters were varied. The variables that had the greatest effect on snow strength were pin size, and snow average grain size.

Part of the motivation of this study was for tire/snow interaction models, so some terramechanics and ground vehicle research was done to ensure that the output of the test data would be in a range that would be useful to those models (Wong, 2001; Lee, 2011).



Our study is a step towards obtaining data at the mesoscale level. Tests on smaller, microscopic scales will discern the properties and orientations of individual snow grains. Tests on larger, macroscopic scales will discern the properties of the bulk snow, where edge effects and size effects have become negligible. Between these, at the mesoscale, representative volume element (RVE) may be defined. The RVE for heterogeneous materials is described in texts on heterogeneous materials (e.g. Nemat-Nasser and Hori, 1999), and is defined as the size at which the strength of snow approaches a constant (i.e. the strength at which the size effect disappears). Although the RVE was not found in this study, these tests were on a scale smaller than the RVE, and larger than the microscopic scale. The concept of an RVE for snow has been suggested by Marshall and Johnson (2009) and Yuan and others (2010).

Most earlier work tackles the larger scale. We examine mm-cm scales and we attempt to extract mechanical properties and deduce size effects at this intermediate scale.

## **2.2 Background**

### **2.2.1 Earlier work**

Previous snow indentation studies have been carried out at larger scales and under different conditions than those utilized here. Seligman (1936) documented indentation tests on seasonal snow, with an eye toward avalanche studies and modeling. Yong and Fukue (1977) performed confined compression tests in natural snows, both fresh and aged, and in artificial snows that were ground from ice. Their samples were cylinders, 5 cm diameter x 4.6 cm high. Edens and Brown (1991) investigated the correlation between microstructure and macrostructural strength by examining morphological changes under snow compression, such

as coordination number, grain size, bond radius, neck length, pore size, free surface area and grains per volume. Shoop and Alger (1998) carried out tests, indenting a 20 cm diameter plate into artificial snow and compared results with a computer modelling study. Additional references on snow indentation can be found in Lee and others (2009).

Other geometries have also been used for indentation testing. These have been based on the Rammsonde cone penetrometer that is also used in geology and soils science (e.g. Gubler, 1975; Dowd and Brown, 1986). The Snow MicroPenetrometer we used for snow characterization has also been used to measure snow strength (Johnson and Schneebeli, 1999; Schneebeli and others, 1999; Marshall and Johnson, 2009). Others have modified the cone to have a round tip (Floyer and Jamieson, 2010).

It has been suggested that there may be some similarities between the mechanical properties of snow and foams, since both are porous, random heterogeneous materials (Kirchner and others, 2001; Yuan and others, 2010). Thus, earlier snow studies and studies on metallic and polymeric foams (Olurin and others, 2000; Andrews and others, 2001; Kirchner and others, 2001; Ramamurthy and Kumaran, 2004; Lu and others, 2008; Flores-Johnson and Li, 2010) are examined here.

Snow has also been described as a bonded granular material (McClung, 1981; Brown, 1994), especially at low, plastic deformation rates. Such deformation rates induce time-dependent ductile failure. Stereology theory is used to calculate the snow strength based on the microstructure, and the time scales are sufficiently long that the snow's metamorphism must be accounted for during deformation. In our study, deformation rates took place in the brittle

region. Kinoshita (1967) provides a discussion of the strain rates that yield ductile vs. brittle failure in snow.

Several different mechanisms for snow deformation are compared and modeled by Mellor (1975) and Johnson and Hopkins (2005).

We apply mathematical models to the laboratory test data. Olurin and others (2000) studied metallic foams under cylindrical indentation, to examine the potential for energy absorption under impact. Flat-bottomed, cylindrical punches were used, and the results from our snow testing, which used similar cylindrical pins, are compared against these results. Andrews and others (2001) studied energy absorption by metallic foams, and performed indentation tests with various geometries. Size effects were examined, and relationships between first peak strengths and pin sizes were determined. The results from our snow tests are compared against these results, as well as results from snow models (Lee, 2009).

Others who have examined the behavior of foams utilising small-scale testing include Onck and others (2001), Ramamurty and Kumaran (2004) and Lu and others (2008). Flores-Johnson and Li (2010) examined the behavior of polymeric foams and Kirchner and others (2001) modeled snow as a foam of ice.

Our study builds upon the earlier work, with the following key features intended for application to ground vehicle traversal:

- Size effects on meso-scales are examined.
- High strain rates are used, so testing occurs fully in the brittle region.
- Natural snows are used.

- Snow selection is based on what is found most commonly in populated regions.
- Flat-bottomed cylindrical indenters are used.

### 2.2.2 Indentation model

The indentation model developed by Lee (2009) uses cohesion, internal friction angle and hydrostatic stress-volumetric plastic strain relationships in a plasticity model to predict stress/displacement curves. The curves are classified into three zones, as shown in a theoretical curve in Fig. 2.

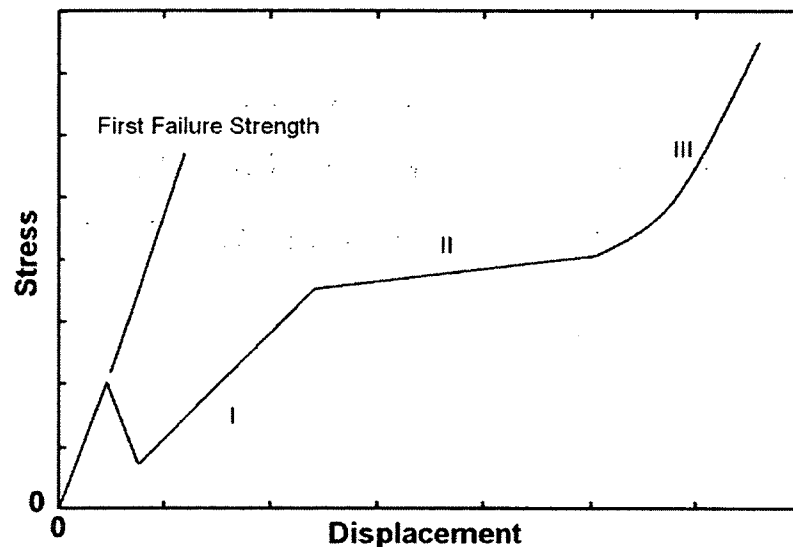


**Fig. 2.** Theoretical stress/displacement relationship for indentation into snow.

First, the stress rises to a peak, before an immediate loss of strength. This first peak is called the first failure strength of the snow. After those first transient effects, the indentation proceeds through three zones discussed in Lee's (2009) model. Zone I exhibits a linear (but plastic) rise in stress as the indenter proceeds through the snow. During Zone I, the indenter

accumulates a densified zone beneath it called a pressure bulb. Muro and O'Brien (2004) cite several papers (e.g. Yosida and others, 1956; Muro and Yong, 1980) that discuss this densification zone. Both a first peak and a densification zone are also mentioned for a round-tipped penetrometer (Floyer and Jamieson, 2010) and for a vertically loaded plate (Shoop and Alger, 1998).

At the transition to Zone II, the pressure bulb has reached its maximum size and it proceeds to move through the snow together with the pin, usually with a slight increase in resistive force due to snow hardening. The average stress during Zone II will, henceforth, be called the "plateau strength".

Zone III is the region where the pressure bulb reaches the bottom of the snow and further compacts. This only occurs during deep indentation, and is provided by the bottom of the snow container in the laboratory, or the frozen soil or street surface in a "real world" application. This is called a densification (finite depth) zone.

### 2.2.3 Plateau strength analysis of foams

Olurin and others (2000) performed similar indentation tests into open-cell aluminum foams and calculated the resistive strength during indentation, separated into two components, a crushing term and a tearing term. The crushing term relates to material being compacted beneath the pin, and is proportional to the leading face surface area. The tearing term relates to the damage to the snow that is caused by the circumferential edge of the pin as it creates new surface while driving into the snow. It is therefore proportional to the pin circumference. Olurin reasoned that:

$$F = F_{crushing} + F_{tearing}$$

$$F = \pi r^2 \sigma_{crush} + 2\pi r \gamma_{tear}$$

$$\frac{F_{PL}}{\pi r} = \sigma_{crush} r + 2\gamma_{tear}$$

where  $F_{PL}$  is the plateau strength (units of force rather than stress),  $r$  is the pin radius and  $\sigma_{crush}$  and  $\gamma_{tear}$  are the crushing and tearing terms respectively. Thus, a plot of  $F_{PL}/(\pi r)$  as a function of pin radius is expected to be linear, with the slope being the crush strength, and the intercept giving the tearing strength.

## 2.3 Experimental procedures

### 2.3.1 Collection and storage of snow

Virgin (undisturbed), metamorphically stable, dry snow was collected in and around Fairbanks, Alaska, in locations far from sources of contamination, at temperatures between -9 and -30°C. Typically, snow was gathered a week after the previous snowfall. This gave adequate time for sufficient metamorphism to provide roughly uniform grains of approximately spherical shape. Air temperature, snow surface temperature and snow pit temperature were recorded at each snow collection site.

Two types of snow were collected. The first was fine-grained (average grain size < 1 mm) snow such as occurs near the surface of a snow pack. This is snow that has fallen within the previous month or so. The second was coarse-grained (average grain size > 1.5 mm) depth hoar such as occurs at depths greater than 20 cm under a surface cover and typically where there is ice over liquid water, such as on a river or a pond. This is snow that has fallen at least three

months earlier, and has been kept at a thermal gradient by exposure to liquid water beneath the ice, and insulated above by fresher snow layers.

Samples were collected in chilled plastic containers and transported to laboratory freezers in a cooler. Laboratory freezers were maintained at  $-30^{\circ}\text{C}$ , cold enough to slow metamorphism and sintering to a very low rate (after six months in storage, little sintering had taken place among the snow grains). Storage time ranged from  $< 1$  day to 6 months.

### 2.3.2 Snow characterization

Snow was selected and characterized both in-situ and in the laboratory using multiple methods, to ensure that snow sample-to-sample variation was minimal. The first in-situ test utilized a high-resolution snow micropenetrometer. Samples were then removed from the snow bank and measured, weighed and sieved on-site to obtain density and grain size distribution. Specimens collected and brought to the laboratory were additionally characterized via optical inspection with a light microscope and CT scanning using 3D X-ray MicroTomography.

The snow micropenetrometer used was developed by Johnson and Schneebeli (1999) for use by avalanche researchers. In this study, it was used to check snow properties in-situ so that appropriate snow samples could be selected. Output of the snow micropenetrometer is penetration force and texture index, which is an empirical number used to describe the snow grain geometry. It is defined as the ratio of mean grain size (mm) to density ( $\text{kg m}^{-3}$ ).

The density was measured at the field collection sites using a graduated cylinder of known mass, hanging from a spring scale. This gave a quick, rough estimate of density that was later compared with the density obtained from the CT scan images.

Grain size distribution was also obtained by sieving, with sieves of 1.4, 1 and 0.425 mm. From this sieving, average grain sizes were estimated to be 1 mm for the fine-grained snow and 2.2 mm for the coarse-grained snow.

CT scanning took place in a cold room, and samples were scanned before and after testing at 23.7  $\mu\text{m}$  resolution using parameters as recommended by Yuan (2007).

The snow micropenetrometer readings, density measurements, weighing and sieving and CT scanning all established baseline microstructures for different natural snows in their natural state, using the International Classification for Seasonal Snow on the Ground (ICSSG; Fierz and others, 2009).

### 2.3.3 Establishment of testing parameters

#### 2.3.3.1 Selection of Snows

We determined that the two snow types occurring with high regularity in aged snow packs in Fairbanks were medium rounded grains near the surface (the top 15 to 20 cm), with coarse faceted rounded particles beneath the fine-grained layer, as described in the ICSSG (Fierz and others, 2009). Measured snow densities ranged from 148 to 251  $\text{kg m}^{-3}$ , with the fine-grained snow generally ranging from 150-170  $\text{kg m}^{-3}$ , and the coarse-grained snow generally ranging from 200-230  $\text{kg m}^{-3}$ . The fine-grained snow had an average grain size  $< 1$  mm, while the coarse-grained snow had an average grain size  $> 1.5$  mm. Texture index values were found to be  $\sim 3$ -4.5 for fine-grained snow, and  $\sim 5$ -7 for coarse-grained snow. Observations and measurements were similar for three consecutive winters, 2008-2009, 2009-2010 and 2010-



2011, enough to instill confidence that test results from snows of different winters were comparable.

### 2.3.3.2 Pin Selection

Cylindrical indenters were chosen because they are most typically used in vehicle-terrain studies. They also have several advantages that make them ideally suited to this study. First, to study size effects, it is necessary to have an indenter for which the size ratios among the different linear dimensions do change with changing indenter size. To illustrate, one of the pieces of data captured in this study was the initial failure strength of the snow, which is a function of initial geometry. The differences among initial geometry due to size are illustrated in Fig. 3.

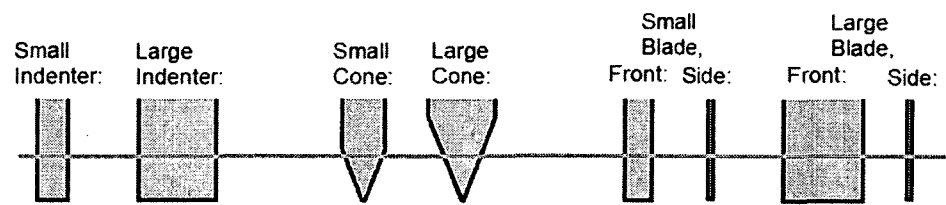


**Fig. 3.** Size effects of different indenter geometries.

Below the green line, a larger radius and a smaller radius cone present the same leading face geometry to the test material (the snow). Therefore, a cone tip test cannot yield a size effect for initial failure strength. A change in cone angle would change the tip geometry, but any differences shown in such a study would be due to a change in angle as well as linear measurements.

For a blade, the linear dimensions change in one direction, but not in the other (the blade thickness). Therefore, a blade test yields a less pronounced size effect for initial failure strength. Other geometric cross sections will work as well as a circular cylinder, but a circular cylinder was chosen to simplify the calculations, and to avoid adding vertical edges.

### 2.3.3.3 Confirmation of Indentation Model Using CT Scans

The CT scan images confirmed that densification did occur during snow indentation. This confirms the theory described in Section 2.2.2 and further discussed in Section 2.4.1. Fig. 4 shows top, front and side cross-sectional views of a column of snow post-indentation. The post-processing of CT scans enables analysis of snow particles slice by slice. Fig. 5 shows a lower slice of a snow sample before and after indentation with a 12.7 mm diameter pin.

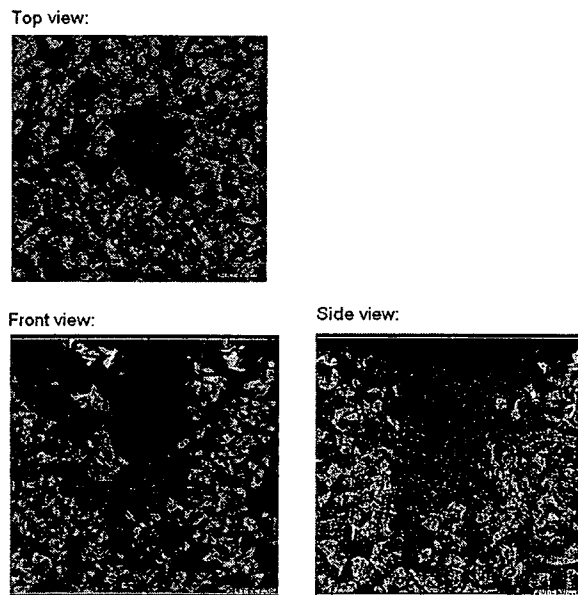


Fig. 4. CT scans of indented snow (white is ice).

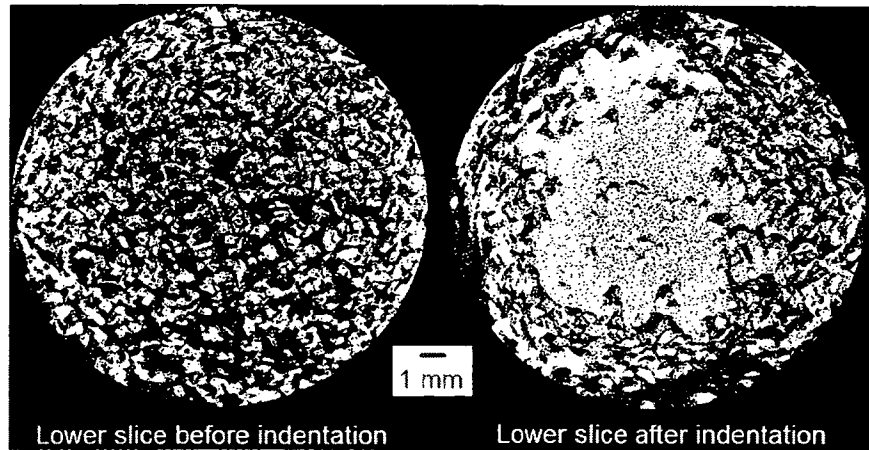


Fig. 5. Cross sections of CT scan of indented snow, 12.7 mm indenter (white is ice).

Using these images, the original density of this snow sample was found to be  $186 \text{ kg m}^{-3}$  (80% porosity), and the density of the region directly beneath the indenter was found to be  $649 \text{ kg m}^{-3}$  (29% porosity). The change in density is indicative of whether the pin is compacting the snow, or drilling through the snow. The larger the pin, the more compaction took place. Fig. 6 shows the comparison for a 6.35 mm pin:

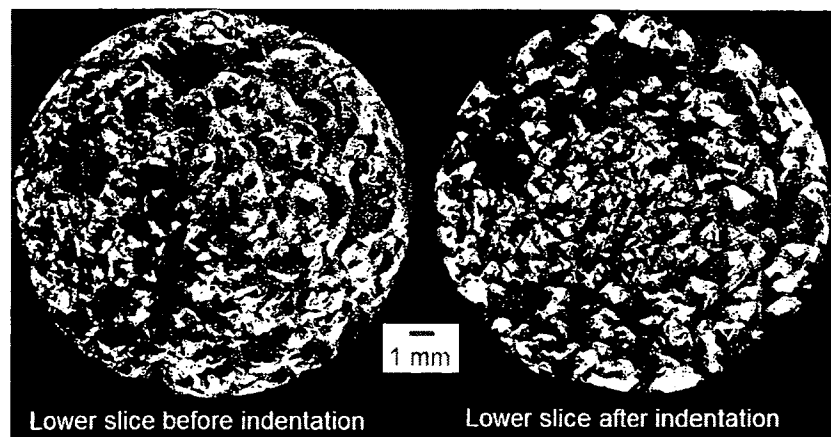


Fig. 6. Cross sections of CT scan of indented snow, 6.35 mm indenter (white is ice).

Using these images, the original density of this sample was  $262 \text{ kg m}^{-3}$  (71% porosity), and the compressed density under the pin after indentation was  $270 \text{ kg m}^{-3}$  (70% porosity). As discussed in Section 2.4.1, less compaction took place with smaller indenter size to average grain size ratio. More compaction can be visually seen in Fig. 5 than in Fig. 6 (the higher percentage of white regions indicates a higher density of ice). Fig. 5 and Fig. 6 are both consistent with the theory, described in Section 2.2.3, of a densification zone beneath the pin.

The CT scanning also provides a criterion for snow container size during testing as follows. From the post-indentation scans, the horizontal slices beneath the indenter were analyzed. For a given snow slice, areal density was measured, of circles and annular regions of increasing size, centered on the spot directly beneath the middle of the indenter. When the density of an annular region was about the density of virgin snow, it was determined that the pressure bulb had been contained within the inner circle. After this test was performed with the largest pin sizes and with a safety factor of 1.5, it was determined that with the container diameter 4 times the pin diameter, containment effects were negligible.

#### 2.3.3.4 Initial Sensitivity Studies

Before formal testing began, sensitivity studies were performed to determine which parameters significantly affected the snow behavior and which did not. After the sensitivity studies were performed, tests were selected to vary only the parameters that would yield results of interest.

Parameters that were varied in the initial sensitivity studies were:

- Snow container diameter: It was found that snow container diameter needed to be at least 4 times the pin diameter in order not to have confinement effects. Confinement effects were determined to be present when an increase in container diameter showed a decrease in apparent snow strength. When a further increase in container diameter showed no apparent change in snow strength, that diameter was determined to be sufficiently large. This was confirmed by CT scanning.
- Snow depth: A depth of 20 mm was chosen because 10 mm was too shallow to achieve the plateau strength, and deeper snow took more time and resources than necessary.
- Indentation depth: Indentation needed to reach zone III in order to achieve results of interest. A depth of 10 mm was chosen because with a snow depth of 20 mm, the first peak and all three indentation zones can be observed within 10 mm of indentation.
- Snow average grain size: No variability due to grain size was observed in the first peak, but differences were observed in zones I and III, so this variation was retained for the formal study.
- Indentation speed: No difference was observed in snow mechanical behavior between indentation speeds of 2 and 5 mm s<sup>-1</sup>, so this variation was removed from the formal study. However, the data that were collected during these tests have proved valuable, so they were kept for analysis.
- Load cell used for test: A small load cell was required for higher sensitivity in the smaller pin tests; a larger load cell was required to cover the range of greater accumulated force in the larger pin tests.

#### 2.3.4 Tribometer setup

A CETR-UMT tribometer was used for indentation testing. This tribometer has high-resolution load cells and is easily adapted to individual tests.

Two different load cells were used for their different capacities: one had a range of 5 - 500 mN and a resolution of 0.05 mN; the other had a range of 2 – 200 N and resolution of 0.01 N. The test region was maintained at a temperature of -20°C using a low-temperature forced air stream, set to an output of -40°C. The reason for this temperature difference is that the enclosure has some inevitable leakage due to the necessity of openings for the various interfaces with the tribometer.

Fig. 7 shows an indentation test in progress (the enclosure was opened only for photography purposes; in actual testing, it remained closed). This example shows a 3.175 mm pin being indented into a small amount of snow. As discussed in Section 2.3.3.3, larger containers were used for the larger pin diameters, to eliminate any confinement effects.



**Fig. 7.** Indentation test setup.

The sample holders were made of flat-bottomed plastic cups to minimize thermal contamination, and the pins were machined of aluminum, which has a good balance of light weight to minimize inertial effects, and high stiffness so that only the effects of the snow are captured during the indentation. In other words, the stiffness of the aluminum was considered to be infinite compared with the stiffness of the snow.

#### 2.3.5 Test parameters

Tests were carried out with the parameters shown in Table 1. Some variations were made due to logistical constraints, and were not part of the variations under study.

**Table 1.** Indentation test parameters

<u>Parameter</u>	<u>Parameters varied for study</u>	<u>Units</u>	<u>Variation part of study?</u>
Indentation pin diameter	3.175, 6.35, 9.525, 12.7, 34, 42	mm	Yes
Indentation depth	10	mm	No
Snow depth	20	mm	No
Indentation speed	2, 5	mm s <sup>-1</sup>	No
Snow type	(1) Fine-grained, average grain size 1 mm, density ranging from 148 to 251 kg m <sup>-3</sup> ; (2) Coarse-grained, average grain size 2.2 mm, density ranging from 200-230 kg m <sup>-3</sup>		Yes
Load cell used for test	200 N capacity with 0.01 N resolution; 500 mN capacity with 0.05 mN resolution		No

Varying different parameters and repeating tests with ambiguous results, ~ 400 Indentation tests were performed in total. Of these, only those that gave clear results and the values needed for a given calculation (e.g. plateau strength for a plateau strength calculation) were used in the data processing.

The ductile-to-brittle transition normal strain rate for snow is about  $10^{-4} \text{ s}^{-1}$  (Kirchner and others, 2001). Strain rates for this set of testing were selected to be well above this strain, but low enough to reduce inertial effects. Thus, all tests were well within the brittle range.

In total, 118 sets of tests were performed, with between 3 and 6 runs of each test. Of these 600-odd data points, ~ 100-200 were used for each data report.



## 2.4 Results

### 2.4.1 Stress-displacement curves

The stress-displacement curves qualitatively reflected the model described in Section 2.2.2. However, not all three zones were present in all cases. The larger the indenter size relative to the average snow grain size, the more distinct the zones. At the limit of very small indenter size to snow grain size ratio, the first peak became unrepeatably as it depended too highly on initial placement of the pin relative to the snow grains. Also, for small indenters, the effect was more that of the pin drilling rather than of the cylinder compressing, and no pressure bulb accumulated, so that Zone I was not represented. At the limit of deep snow, where the pressure bulb did not contact the bottom surface, Zone III did not occur. At the limit of very shallow snow, Zone II was not represented because the pressure bulb hit the bottom before it attained its maximum size.

Fig. 8 shows the stress-displacement relationship for four 12.7 mm pin indentations into fine-grained snow. The horizontal axis is the pin displacement into the snow. The vertical axis is the stress, i.e. the resultant force detected by the load cell coupled to the pin, divided by the cross-sectional area of the pin.

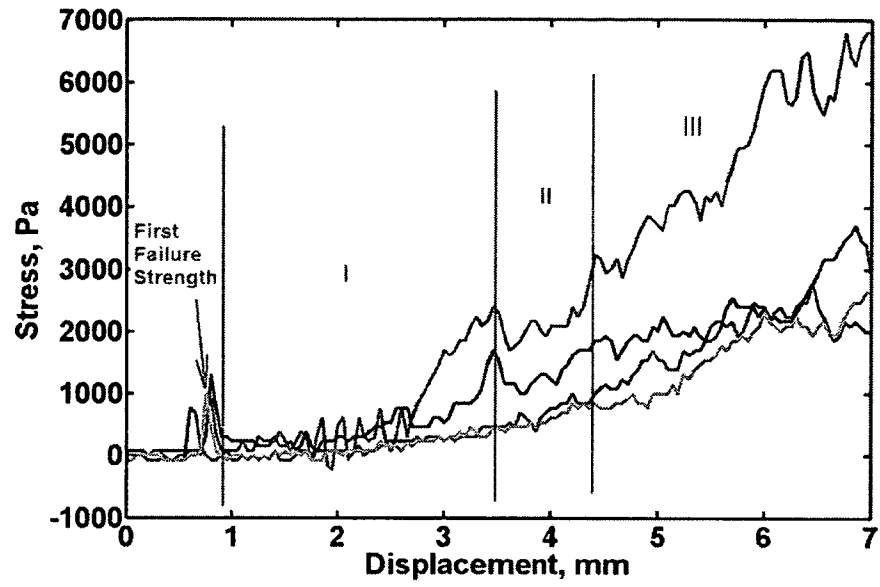


Fig. 8. Stress-displacement curves for 12.7 mm pin indentations into fine snow.

Fig. 9 shows the stress-displacement relationships for two different pin sizes and two different snow types.

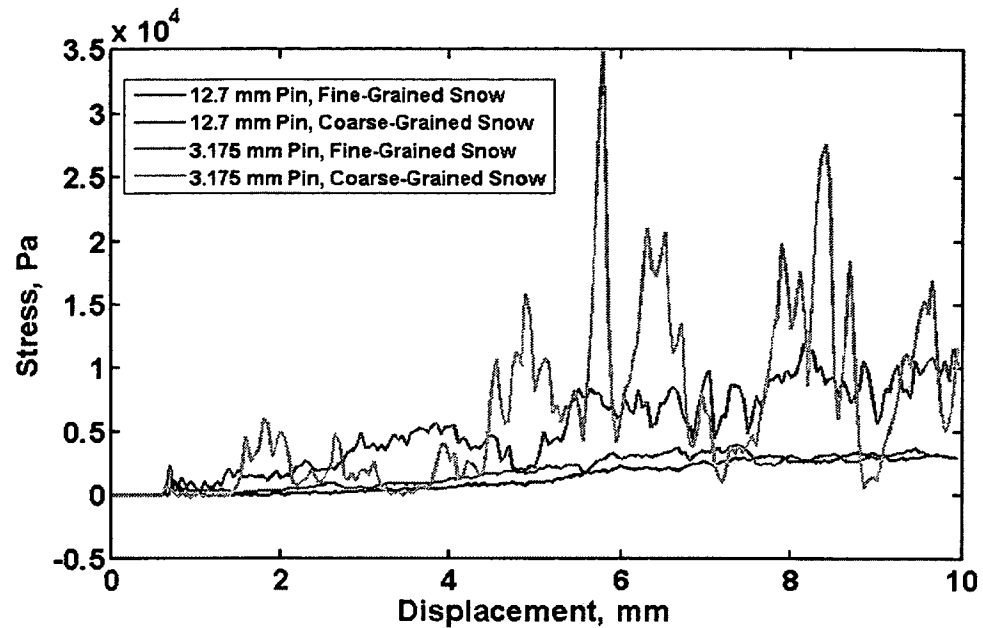


Fig. 9. Stress-displacement curves comparing pin sizes and snow types.

As will be discussed in Sections 2.4.2 and 2.4.3, the overall forces are higher for the smaller pin. It is also qualitatively observed that Zones I and III do not occur for the 3.175 mm pins, since snow was not compacted in those tests. The curves show a transition from the initial peak directly to Zone II. Moreover, we observe that the 3.175 mm indentation into fine-grained snow yielded a smoother curve than the indentation into the coarse-grained snow, because the pin was large enough with respect to the grain size to read an average force over multiple snow grains. In contrast, the indentation into coarse-grained snow yielded a much less consistent force because the indenter size was on the same order of magnitude as the snow grain size. Thus the behavior of individual snow grains was detected.

Fig. 10 shows the same 12.7 mm indentation data as in Fig. 9, but with the 3.175 mm data removed so that the detail of the larger pin indentation may be seen.

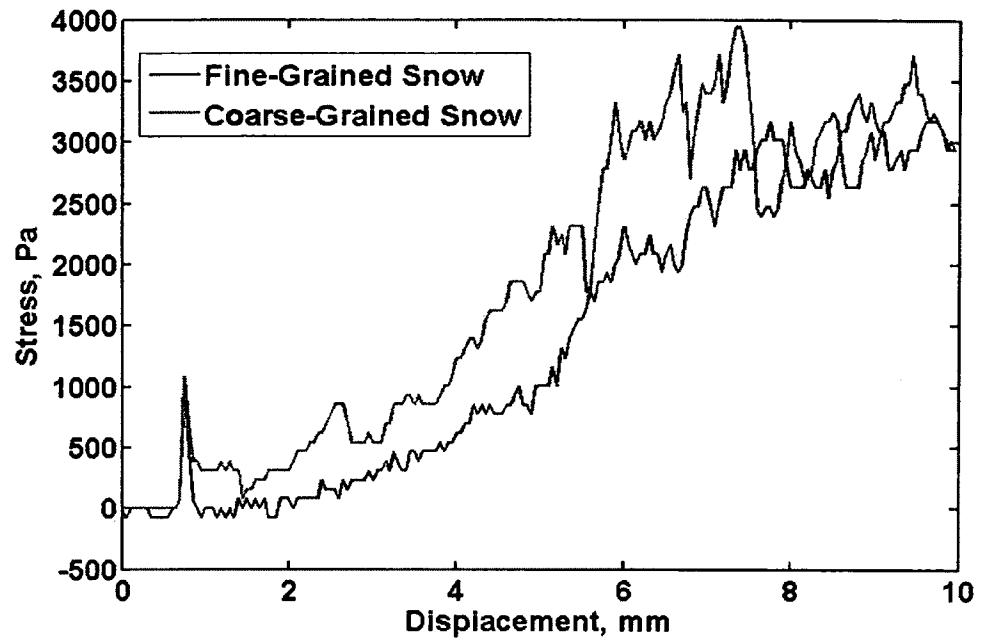


Fig. 10. Stress-displacement curves for 12.7 mm pin indentations, comparing two snow types:

Here, where the indenter size is sufficiently large that the ratio of indenter size to snow grain size  $\gg 1$  in both cases, both graphs look similar.

#### 2.4.2 First peak strength

The size of the indenter and the average grain size of the snow were varied to determine their effects on first peak strength. It was found (Fig. 11) that the larger the indenter, the lower the first peak failure strength. On  $\log_e$  scales, a linear relationship is evident so that a power law is apparent:

$$\sigma_{fs} = kA^{-\gamma},$$

where  $\sigma_{fs}$  is the failure stress,  $\gamma$  is a dimensionless material property,  $A$  is the pin area and  $k$  is a constant.

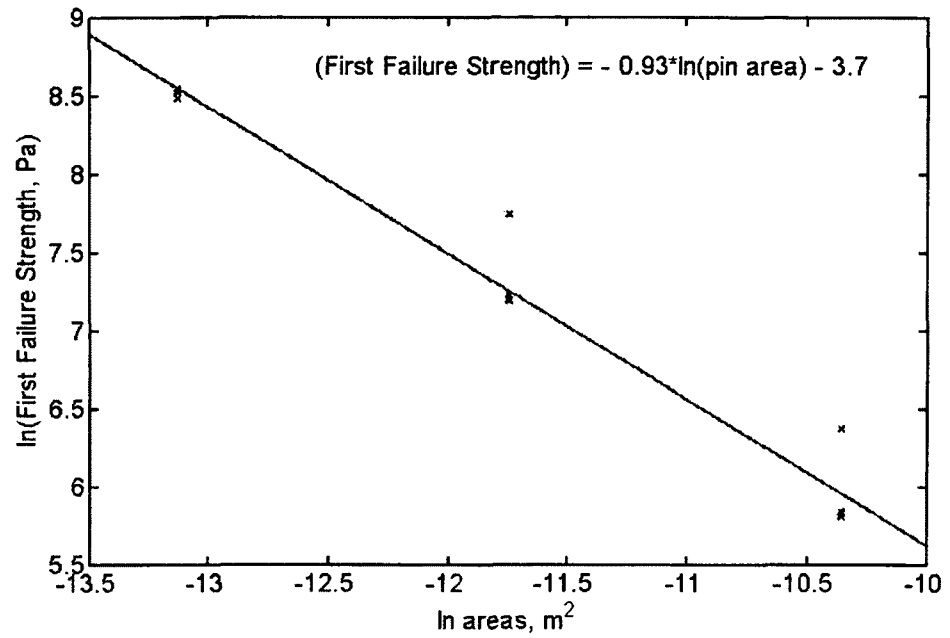


**Fig. 11.** Example of first failure strength data, fine-grained snow.

Table 2 shows results obtained for  $\gamma$  against other parameters. Each test ID represents 4-6 indenter sizes, with 3-6 indentations repeated for each size.

**Table 2.** Exponent from a range of tests.

<u>Test ID Number</u>	<u>Test Date</u>	<u>Snow Type</u>	$\gamma$
0	09 July 14	Fine-grained, collected March 2009	.97
2	09 Dec 30	Fine-grained, collected December 2009	.62
3	10 Jan 06	Fine-grained, collected December 2009	.92
4	10 Jan 16	Fine-grained, collected December 2009	.76
6	11 Mar 18	Fine-grained, collected December 2010	.93
7	11 Mar 18	Fine-grained, collected December 2010	.80
1	09 July 14	Coarse-grained, collected March 2009	.98
5	10 Jan 16	Coarse-grained, collected March 2009	.71

The average value of  $\gamma$  is 0.83 (with a coefficient of variation of 0.16) for fine-grained snow, and 0.85 (with a coefficient of variation of 0.23) for coarse-grained snow. The average value for both snow types is 0.84, with a coefficient of variation of 0.16.

The actual values of first peak strength had high test-to-test variability (as high as an order of magnitude), even when the same snow sample was used, and all other test conditions were ostensibly the same. The source of this variability is not understood, but it is specific to the first peak strength values over time. On the same day, first peak strength values were highly repeatable. Also, plateau strength values (Section 2.4.3) did not show the same day-to-day variability. However, all the different sets of data yielded the fairly consistent values of  $\gamma$  shown in Table 2.

The other size relationship explored was that of grain size. Identical tests were performed on both fine- and coarse-grained snow. The first peak strengths had the same mean

values and same coefficients of variation for both fine- and coarse-grained snow, although grain size did affect other snow properties as discussed in Section 2.4.1.

### 2.4.3 Plateau strength (zone II)

The mean plateau strengths for several different test sets are given in Table 3, in which ~150 tests are represented with each test yielding one data point. Typical results are shown in Table 3. Each pin diameter in each test set was tested 4 times, but not all gave a measurable plateau.

**Table 3.** Mean plateau strengths from a range of tests.

<u>Pin diameter (mm)</u>	<u>Mean plateau strength for fine-grained snow (Pa)</u>	<u>Coefficient of variation for fine-grained snow (unitless)</u>	<u>Mean plateau strength for coarse-grained snow (Pa)</u>	<u>Coefficient of variation for coarse-grained snow (unitless)</u>
1.588	15700	0.63	No test performed	No test performed
3.175	5620	0.74	6010	0.67
6.350	6940	0.78	4010	0.69
9.525	5800	1.06	3360	0.64
12.700	2560	0.21	3000	0.31

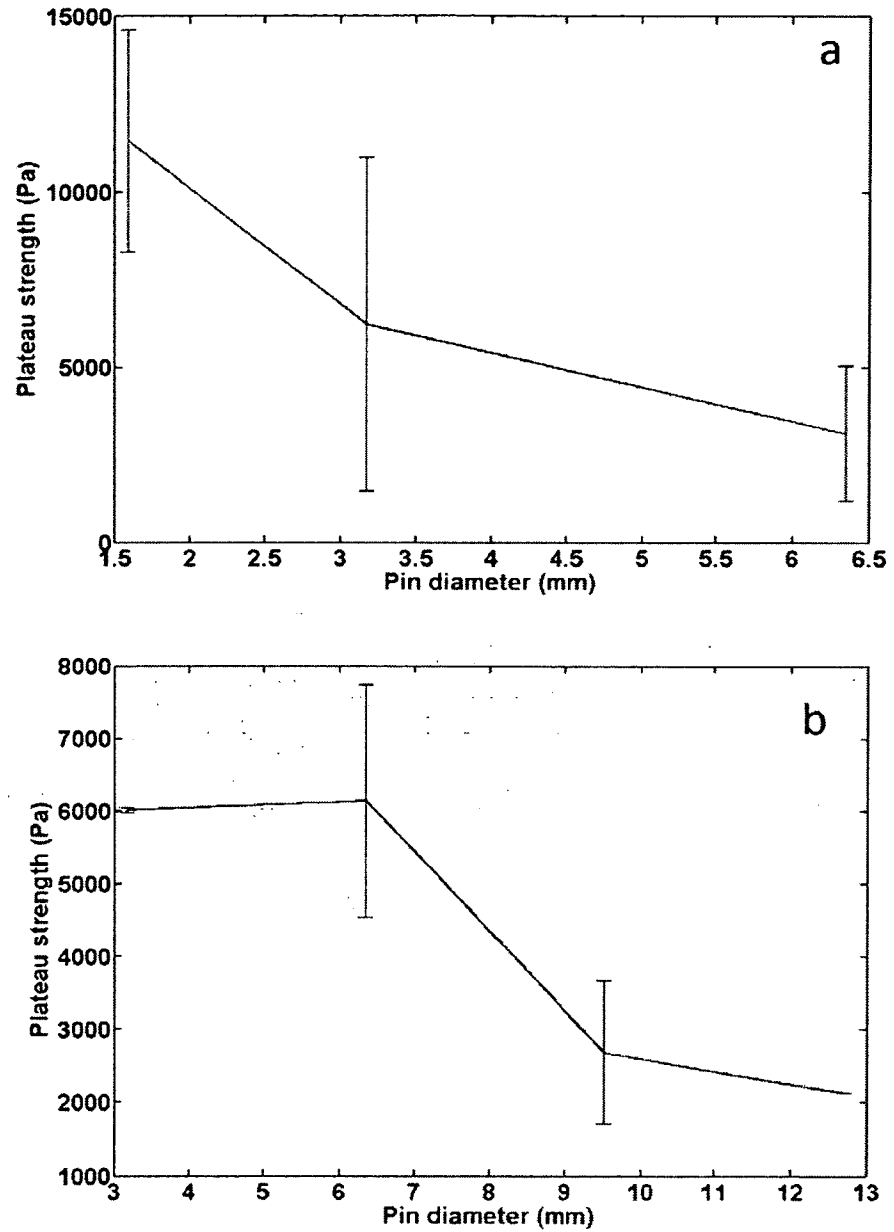
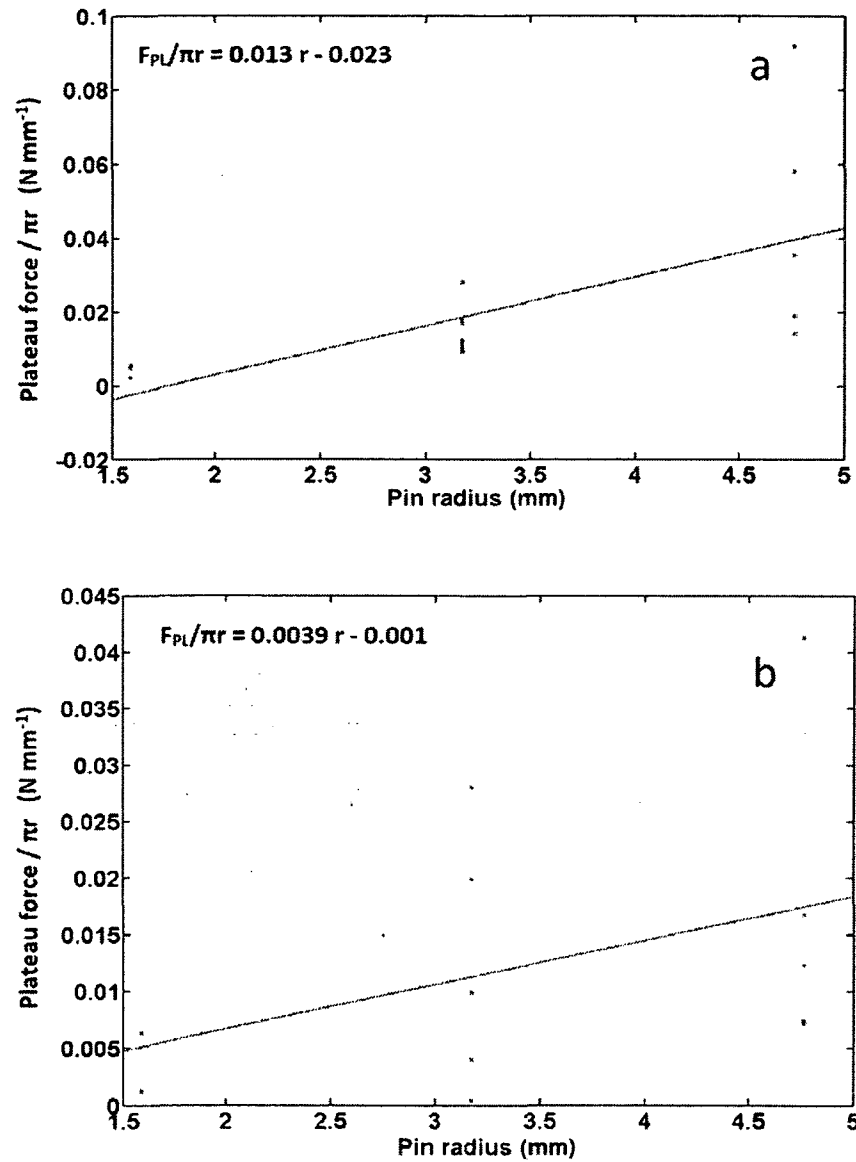


Fig. 12. Relationship between plateau strength and pin diameter, for (a) fine grained snow and (b) coarse-grained snow (there is only one data point at 12.7 mm).



About three quarters of the plateau strengths were determined "semi-automatically", by criteria that were based on the specific test run. The plateau was defined by the rule: "when the moving average of X points changes by more than Y and remains stable for Z data points, then Z is called the plateau." X, Y and Z were manually selected on a test-by-test basis, due to the large test-to-test variation. A quarter of the resulting plateau strengths came out completely inappropriately; plateau ranges were hand-selected using careful visual judgment.

The raw data for the plateau strengths shows a monotonically decreasing trend with increasing diameter. With such a large spread and with only four different diameters yielding plateau strengths, the mathematical form of the relationship is difficult to determine. However, once the data are analyzed for material properties as discussed in Section 2.2.3, the plot output from those calculations is much more useful. Representative results of plateau force,  $F_{PL} / \pi r$  (c.f. Section 2.3) for two different test sets are shown in Fig. 13. All test sets reflect multiple days of testing, often in different years, so the spread of data is quite large. However, this enabled more data points to be used, ensuring broad representation. Each data point represents one test.



**Fig. 13.** Plateau force /  $\pi r$  as a function of pin radius at  $2 \text{ mm s}^{-1}$  for (a) fine-grained and (b) coarse-grained snow.

Results from the four data sets that displayed a linear trend are shown in Table 4, in which  $\sim 150$  tests are represented with each test yielding one data point. The apparent negative

values of the shear term can be taken to be zero. This seems to indicate that the tearing term is indeed negligible.

**Table 4.** Compaction and shear terms from a range of tests.

<u>Test ID</u>	<u>Snow average grain size (mm)</u>	<u>Mean value of compaction term, <math>\sigma_{crush}</math> (kPa)</u>	<u>Mean value of shear term, <math>2v_{tear}</math> (<math>N\ mm^{-1}</math>)</u>
1	1.0	13	-0.023
2	1.0	3.0	0.0058
3	2.2	3.9	-0.001
4	2.2	3.8	-0.0021

#### 2.4.4 Absorption of energy

Total energy absorption for each indentation, from first contact with the snow to the completion of the test (in this case, 10 mm indentation), was calculated by taking the area under the force-displacement curve. The entire curve was used because energy absorption, unlike first peak strength or plateau strength, is a property that is cumulative with indentation depth. The deeper the snow, the more stable (with respect to depth) is the measured energy absorption density, since the transient initial effects from the first peak and Zone I become much smaller than the effects from the plateau region of Zone II.

To normalize against geometric factors and arrive at a dimensionless number, the volumetric absorbed energy density was calculated by dividing the absorbed energy by the volume of snow displaced and by Young's Modulus for ice, for which we used 9 GPa (Schulson, 1999. Fig. 14 shows results from all tests, of energy absorption density, with no outliers

removed. Some smaller scatter was expected in these data due to the cumulative nature of the calculation of the energy absorption. Note that energy absorption data could be collected for the two largest pin sizes, 34 and 42 mm, yet data for these two pin sizes yielded neither a first peak, nor a plateau strength. Additionally, note that fine-grained snow showed a greater amount of scatter than coarse-grained snow. This indicates a greater variability of snow behavior in fine-grained snow than coarse-grained.

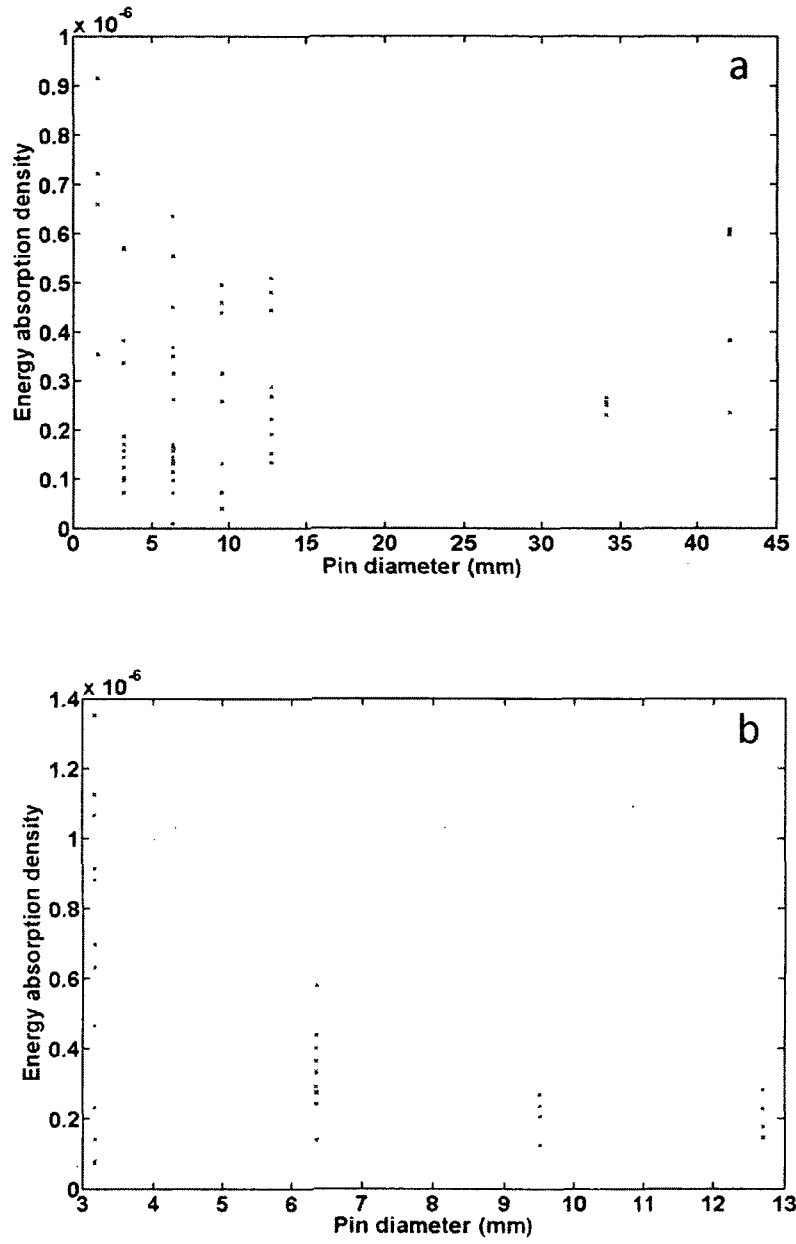


Fig. 14. Energy absorption density during pin indentation into (a) fine-grained and (b) coarse-grained snow.

It was found that the average energy absorption density was  $3.4 \times 10^{-7}$  for fine-grained snow, and  $4.1 \times 10^{-7}$  for coarse-grained snow. These results suggest that for cylindrical indentation in this size range, energy absorption density was constant with respect to diameter for fine-grained snow, and decreased with increasing diameter for coarse-grained snow. Note that this decrease was not linear, flattening out to suggest energy absorption independence of size at larger diameters.

## **2.5 Discussion**

### **2.5.1 First peak strength**

First peak snow strength was highly dependent upon surface conditions and showed high test-to-test variation. Even when known factors were carefully controlled, a different day would yield different first peak strengths, even though the spread of first peak data for a given day was very small. This suggested variations were due not to the equipment or operator, but to intrinsic changes that occur in the surface properties of the snow with storage time. The variability between tests was much smaller for plateau strengths, suggesting that changes that led to the high variability in initial failure strength did not affect snow behavior beyond the first failure. Once the pressure bulb had accumulated, the bulb itself exhibited volumetric properties that were consistent from test to test. By the time the test had reached Zone II, the transient effects of the initial conditions had effectively disappeared and the plateau strength better reflected the intrinsic properties of the snow.

The value of the exponent in the power law relationship between first peak strength and pin area was consistent from snow sample to snow sample, so although the absolute first peak strength was highly sample-dependent, the magnitude of the size effect was consistent.

The average value of the power law exponent for both snow types is 0.84. As a comparison, the exponent for brittle foams was estimated to be 0.5 (Gibson and Ashby, 1999), lower than that for the snow tested, indicating that the size effect displayed by first peak strength in snow is greater than that for brittle foams.

#### 2.5.2 Plateau strength

The plateau strengths used to calculate the crush strength of snow were repeatable and are believed to reflect fundamental properties of the bulk snow. The plateau strength is also of more use to engineers and scientists, as it is reasonable to expect a tire, ski, sled runner, animal paw or hoof to compress the snow a small amount before coming to a stop after a certain compression amount. What limits this compression amount is of more interest than the initial collapse strength.

Olurin and others' (2000) values for  $\sigma_{\text{crush}}$  for aluminum foam range from 1.4 to 2.8 MPa. Data for the bulk material properties of *Alporas*, the trade name for the aluminum foam used in Olurin's studies, could not be found, but the ultimate strength of a few randomly selected brittle aluminum alloys on [www.matweb.com](http://www.matweb.com) are in the 500 MPa range. The ultimate brittle failure strength of water ice, in comparison, is about 10 MPa (Gold, 1977). The ratio of ultimate failure strength of bulk material to crush strength of associated foam is 2 orders of magnitude for aluminum/aluminum foam and 4 orders of magnitude for ice/snow. Although a direct

comparison cannot be made because the exact material properties of bulk *Alporas* are unknown, it seems reasonable that the ratio of snow strength to ice strength be lower than the ratio of metal foam strength to bulk metal strength, because snow is formed from ice crystals sitting in contact, with perhaps some but certainly no guaranteed, sintered bonds between individual crystals. *Alporas* foam, in contrast, is formed by injecting air bubbles into a molten metal matrix, then cooling it (Miyoshi and others, 2000). This is counter to ice, and in theory, the metal matrix could have the same crystal structure as the bulk metal. It is also of interest to note that for the snow density range studied here, the ratio of snow tensile strength to that of ice can be very small as summarized by Petrovic (2003).

Despite the higher test-to-test repeatability and fundamental nature of the plateau strength, it still exhibits considerable scatter. This is to be expected from a natural, non-engineered material. Smaller scatter has been obtained for artificial snows (Shoop and Alger, 1998). Differences in mechanical performance among natural, sorted and artificial snows are discussed by Yong and Fukue (1977). The literature on synthetic foams also exhibits very little scatter in engineered materials (Andrews and others, 2001; Ramamurty and Kumaran, 2004; Lu and others, 2008; Flores-Johnson and Li, 2010).

### 2.5.3 Energy absorption

Coarse-grained snow exhibited decreasing energy absorption ability with increasing indenter diameter. This decrease was not linear, flattening out to suggest energy absorption independence of size at larger diameters. Fine-grained snow showed much greater scatter, suggesting there was greater variability of absorption capabilities with different samples than for coarse-grained snow. This could be because snow collection of fine-grained samples took



place over many months (November through March of each boreal season), with much more potential for varying snow conditions, while collection of coarse-grained samples only occurred in March, allowing less variation.

## 2.6 Conclusions

Mechanical indentation testing of snow has provided results consistent both from test to test and from one snow season to another.

Strength tests on snow indicate a power law decrease of first peak failure strength with increasing indenter diameter. The average value of the power law exponent was 0.83 for fine-grained snow and 0.85 for coarse-grained snow. The average value over both snow types was 0.84 with a coefficient of variation of 0.16.

The average plateau strength decreased with increasing diameter, and the data presented here ranged from 3100 to 7500 Pa. Following the example of Olurin and others (2000), plateau strength values were used to calculate the crush strength of the snow, which ranged from 3 to 13 kPa, and the tearing strength, which was determined to be negligible.

The average energy absorption densities were constant with respect to indenter size for fine-grained snow, and decreased with increasing indenter size for coarse-grained snow but may become independent of indenter size at sufficiently large diameter. We found average energy absorption density was  $3.4 \times 10^{-7}$  for fine-grained snow and  $4.1 \times 10^{-7}$  for coarse-grained snow.

We have attempted to extract properties of pure, dry, undisturbed snow. In nature, snow is subject to other forces and factors, e.g. wind, impurities, temperature fluctuations and

humidity. These factors need to be taken into account as they affect snow's intrinsic strength and its surface properties.

For engineering applications additionally, if the interfacing material of interest, e.g. tire rubber, is pliant, the properties of the interfacing material need to be taken into account along with the properties of the snow.

It must also be noted that the size effects discussed here have only been tested on the scales reported, and should not be extrapolated beyond the end points of the data presented here.

The key conclusions from this study are:

1. First peak failure strength for snow exhibits a power law decrease with increasing indenter diameter.
2. The power law exponent for the relationship between first peak failure strength and indenter diameter is highly repeatable.
3. Plateau strength for snow decreases with increasing indenter diameter, and is a more fundamental characterization of snow than first peak strength.
4. Material properties concerning crushing strength can be calculated from the plateau strength. Tearing strength is negligible.
5. Energy absorption density decreases with increasing indenter diameter in small size ranges, and is independent of indenter diameter above a certain minimum size.

**Acknowledgements**

We gratefully acknowledge support for this work by the U.S. Army TACOM Life Cycle Command under Contract No. W56HZV-08-C-0236, through a subcontract with Mississippi State University. This work was performed in part for the Simulation Based Reliability and Safety (SimBRS) research program. Any opinions, findings and conclusions or recommendations expressed in this material are those of the authors and do not necessarily reflect the views of the U.S. Army TACOM.

Disclaimer: Reference herein to any specific commercial company, product, process, or service by trade name, trademark, manufacturer, or otherwise, does not necessarily constitute or imply its endorsement, recommendation, or favoring by the United States Government or the Department of the Army (DoA). The opinions of the authors expressed herein do not necessarily state or reflect those of the United States government or the DoA, and shall not be used for advertising or product endorsement purposes.

## References

- Andrews, E.W., G. Gioux, P. Onck and L.J. Gibson 2001. Size effects in ductile cellular solids. Part II: experimental results. *International Journal of Mechanical Sciences*, **43**(3): 701-713.
- Brown, R.L. 1994. *Changes in Microstructural Parameters of Snow during Deformation*. Montana State University Bozeman.
- Dowd, T. and R.L. Brown 1986. A New Instrument for Determining Strength Profiles in Snow Cover. *Journal of Glaciology*, **32**(III): 299-301.
- Edens, M.Q. and R.L. Brown 1991. Changes in Microstructure of Snow under Large Deformations. *Journal of Glaciology*, **37**(126): 193-202.
- Fierz, C., R.L. Armstrong, Y. Durand, P. Etchevers, E. Greene, D.M. McClung, K. Nishimura, P.K.S. Satyawali and S.A. Sokratov 2009. *The International classification for seasonal snow on the ground*. Technical documents in Hydrology, **83**: 90 p.
- Flores-Johnson, E.A. and Q.M. Li 2010. Indentation into polymeric foams. *International Journal of Solids and Structures*, **47**(16): 1987-1995.
- Floyer, J. and J. Jamieson 2010. Rate effect experiments on round-tipped penetrometer insertion into uniform snow. *Journal of Glaciology*, **56**(198): 664-672.
- Gibson L.J. and M.F. Ashby. 1999 *Cellular solids: structure and properties*, 2nd edn. Cambridge University Press, Cambridge
- Gold, L.W. 1977. Engineering Properties of Fresh-Water Ice. *Journal of Glaciology*, **19**(81): 197-212.
- Gubler, H.U. 1975. On the Rammsonde Hardness Equation. *Proceedings of the Grindewald Symposium*, 114: 110-121.

- Jellinek, H.H.G. 1957. Compressive Strength Properties of Snow. *Journal of Glaciology*, **3**(25): 345-354.
- Johnson, J.B. and M.A. Hopkins 2005. Identifying microstructural deformation mechanisms in snow using discrete-element modeling. *Journal of Glaciology*, **51**(174): 432-442.
- Johnson, J.B. and M. Schneebeli 1999. Characterizing the microstructural and micromechanical properties of snow. *Cold Regions Science and Technology*, **30**(1-3): 91-100.
- Kinosita, S. 1967. Compression of snow at constant speed. *Proceedings of the International Conference on Physics of Snow and Ice*, Sapporo, Japan.
- Kirchner, H.O.K., G. Michot, H. Narita and T. Suzuki 2001. Snow as a foam of ice: Plasticity, fracture and the brittle-to-ductile transition. *Philosophical Magazine A*, **81**(9): 2161 - 2181
- Lee, J.H. 2009. A new indentation model for snow. *Journal of Terramechanics*, **46**(1): 1-13.
- Lee, J.H. 2011. An Improved Slip-Based Model for Tire/snow Interaction. *SAE International Journal of Materials and Manufacturing*, **4**(1): 278-288.
- Lee, J.H., D. Huang, H.P. Marshall and J.B. Johnson 2009. Microscale Direct Simulation of Snow Penetration Tests and Inversion of Signals. *11th European Regional Conference of the International Society of Terrain Vehicle Systems*, Bremen.
- Lu, G., J. Shen, W. Hou, D. Ruan and L.S. Ong 2008. Dynamic indentation and penetration of aluminium foams. *International Journal of Mechanical Sciences*, **50**(5): 932-943.
- Marshall, H.P. and J.B. Johnson 2009. Accurate inversion of high-resolution snow penetrometer signals for microstructural and micromechanical properties. *Journal of Geophysical Research-Earth Surface*, **114**(F4), F04016

- McClung, D.M. 1979. Failure Characteristics of Alpine Snow in Slow Deformation. *International Symposium on the Mechanical Behaviour of Structured Media, Ottawa, Canada*, Elsevier Scientific Publishing Company, Amsterdam, 409-418.
- Mellor, M. 1974. A Review of Basic Snow Mechanics. U.S. Army Cold Regions Research and Engineering Laboratory.
- Miyoshi, T., M. Itoh, S. Akiyama and A. Kitahara 2000. ALPORAS Aluminum Foam: Production Process, Properties, and Applications. *Advanced Engineering Materials*, **2**(4): 179-183.
- Muro, T. and J. O'Brien 2004. *Terramechanics; Land Locomotion Mechanics*. A.A. Balkema Publishers.
- Muro, T. and R.N. Yong 1980. Rectangular Plate Loading Test on Snow - Mobility of Tracked Oversnow Vehicle. *Journal of the Japanese Society of Snow and Ice*, **42**(1): 17-24.
- Nemat-Nasser, S. and M. Hori 1999. *Micromechanics: Overall Properties of Heterogeneous Materials*. 2nd ed., North Holland.
- Olurin, O.B., N.A. Fleck and M.F. Ashby 2000. Indentation resistance of an aluminium foam. *Scripta Materialia*, **43**(11): 983-989.
- Onck, P.R., E.W. Andrews and L.J. Gibson 2001. Size effects in ductile cellular solids. Part I: modeling. *International Journal of Mechanical Sciences*, **43**(3): 681-699.
- Petrovic, J.J. 2003. Review Mechanical properties of ice and snow. *Journal of Materials Science*, **38**(1): 1-6.
- Ramamurty, U. and M.C. Kumaran 2004. Mechanical property extraction through conical indentation of a closed-cell aluminum foam. *Acta Materialia*, **52**(1): 181-189.

- Schneebeli, M., C. Pielmeier and J.B. Johnson 1999. Measuring snow microstructure and hardness using a high resolution penetrometer. *Cold Regions Science and Technology*, **30**(1-3): 101-114.
- Schulson, E.M. 1999. The structure and mechanical behavior of ice. *Journal of the Minerals Metals and Materials Society*, **51**(2): 21-27.
- Seligman, G. 1936. *Snow structure and ski fields: Being an account of snow and ice forms met with in nature, and a study on avalanches and snowcraft*. Macmillan and Co., London.
- Shoop, S.A. and R. Alger 1998. Snow Deformation Beneath a Vertically Loaded Plate: Formation of Pressure Bulb with Limited Lateral Displacement. *Proceedings, ASCE Cold Regions Specialty Conference*.
- Wong, J.Y. 2001. *Theory of Ground Vehicles*. 3rd ed. Wiley, New York
- Yong, R.N. and M. Fukue 1977. Performance of Snow in Confined Compression. *Journal of Terramechanics*, **14**(2): 59-82
- Yosida, Z., H. Oura, D. Kuroiwa, T. Hujioaka, K. Kojima, S. Aoi and S. Kinoshita 1956. Physical Studies on Deposited Snow, II. Mechanical properties. *Contributions from the Institute of Low Temperature Science, Hokkaido University*, **9**(1): 1-81.
- Yuan, H. 2007. *Stochastic reconstruction of snow microstructure from x-ray microtomography images*. University of Alaska Fairbanks, Fairbanks, AK
- Yuan, H., J.H. Lee and J.E. Guilkey 2010. Stochastic reconstruction of the microstructure of equilibrium form snow and computation of effective elastic properties. *Journal of Glaciology*, **56**(197): 405-414.

### 3 Mechanical properties of snow using compression tests: size effects<sup>2</sup>

Daisy HUANG, Jonah H. LEE

**ABSTRACT.** Intrinsic mechanical properties of snow without edge and shear effects may be obtained by performing unconfined compression tests on free-standing snow cylinders. Consistent snows were selected and allowed to sinter before testing, and the stress vs. displacement curves yielded numbers for an initial and a plateau strength value. Energy absorption for each cylinder was also calculated. The initial strength, the plateau strength, and the energy absorption capacity all showed a linear increase with increasing aspect ratio.

#### 3.1 Introduction

Understanding the mechanical response of snow on the ground via quantitative measurement is important to many scientific and engineering applications. Snow may be regarded as an engineering material, with most of the standard material properties (yield strength, ultimate strength, Young's modulus, etc.) measurable and quantifiable using various tests such as indentation (Huang and Lee, 2013), triaxial (Lang and Harrison, 1995), and compression tests.

Indentation tests have been used extensively in vehicle-snow interaction studies to obtain pressure-displacement relationships (Jellinek, 1957; Yong and Fukue, 1977; Edens and Brown, 1991; Shoop and Alger, 1998). Our prior paper (Huang and Lee, 2013) discussed the results of meso-scale (mm-cm) indentation testing and summarized the size effects inherent in snow. However, unconfined compression tests are also of interest because they remove the

---

<sup>2</sup> Huang, D. and J.H. Lee, Journal of Glaciology, submitted Feb. 6, 2013



circumferential effects, if any, inherent in a pin indentation. Where indentation tests relate to a material's hardness and toughness, unconfined compression tests relate to a material's bulk ability to resist stress. Size effects are also examined in this study, with varying diameters, heights, and aspect ratios. Because in tire-snow interactions, the tire and its tread are in contact with the snow on varying length scales, the study of the size effect of snow is thus important for both materials science and application.

Prior studies of compression tests using snow have been done, but on larger scales and with different goals. Jellinek (1957) examined the compressive strength of snow cylinders as a function of age of snow, grain size, and age of cylinders. His cylinders measured  $\Phi$  4.38 cm x 25 cm high and were compressed before aging and testing. Jellinek and his team formed relationships between the snow's thermal history and its current mechanical properties. Our study uses similar methodology, but we are interested not in how the thermal history is related to the current material properties, but rather how current, measureable, known geometries can be used to predict current strength. Fukue and Yong (1979) performed compression tests in natural snows, both fresh and aged, and in artificial snows that were ground from ice. The sample size that they used was  $\Phi$  5 cm x 4.6 cm high. Edens and Brown (1991) probed into the correlation between microstructure and macrostructural strength by examining morphological changes under snow compression, such as coordination number, grain size, bond radius, neck length, pore size, free surface area, and grains per volume.

Part of the motivation of this study was for tire-snow interaction models, so some terramechanics and ground vehicle research was done to ensure that the output of the test data would be in a range that would be useful to those models (Wong, 2001; Lee, 2011).

This current study is a step toward filling in data at the mesoscale level. The prior work was all done with much larger snow samples. In this study, mm-cm scales are used, and an attempt is made to extract mechanical properties at this scale. Our earlier work on indentation testing (Huang and Lee, 2013) was also built upon for this study, and the same snow sampling techniques and methodologies were used. Results for the compression tests are compared with those for the indentation tests, when appropriate, to gain additional insight on the intrinsic mechanical properties of snow. In addition, in materials science, compression tests of semi-brittle porous materials are usually more difficult than tensile tests due to the possibilities of multiple failure modes (Bazant and Xiang, 1997; Tang and others, 2005), the failure patterns of the compression tests are also reported in this paper.

The mechanical properties of snow depend on microstructure, influenced by environmental conditions over time. In order to obtain the results that are most fundamental to pure snow crystals, this study uses dry, virgin, metamorphically stable snow that has been gathered in areas remote from roads and other sources of contamination. The type of snow selected is the stage of a snowpack after it has fallen in cold, dry temperatures, and has had little to no exposure to wind, humidity, thermal cycling, nor contaminants. In Fairbanks, Alaska such metastable snow is available for most of the duration of long, cold, dry, windless winters.

### **3.2 Experimental procedures**

In this section, the sampling of snow is first described followed by test setup and parameters.

### 3.2.1 Selection, collection, and storage of snow

The snow samples collected were clean, dry, and sufficiently aged to have stabilized in their metamorphosis. Such snow samples had nearly uniform rounded grains of consistent density and grain size distribution. The criteria used for snow sample selection are described in the International Classification for Seasonal Snow on the Ground (ICSSG; Fierz and others, 2009). Details on the snow characterization and selection have been previously reported in (Huang and Lee 2013).

### 3.2.2 Instron setup for unconfined compression testing

Unconfined compression testing requires the snow samples to maintain their shape without confinement. Thus the samples were allowed to sinter in cups with flat bottoms and 90° walls at prescribed diameters and heights at a temperature close to melting (-10° C) for five days. After the sintering, the snow samples would hold their shape when removed from their containers and would be used in testing immediately.

The Instron 4466 was used for unconfined compression testing. The Instron Company makes its own cold temperature chamber, which cools using compressed CO<sub>2</sub> gas. The temperature of the testing region was maintained at -20° C.

The snow samples were tested by placing a given snow plug onto a chilled steel platen inside the cold temperature chamber, and a second chilled steel platen, which was coupled to the Instron load cell, was lowered onto the snow plug. Steel was selected due to its high stiffness, which is essentially infinite when compared with stiffness of snow, so that only the

properties of the snow would be captured. Fig. 15 shows an unconfined compression test taking place. The door was opened for photography purposes only; it remained shut during testing.

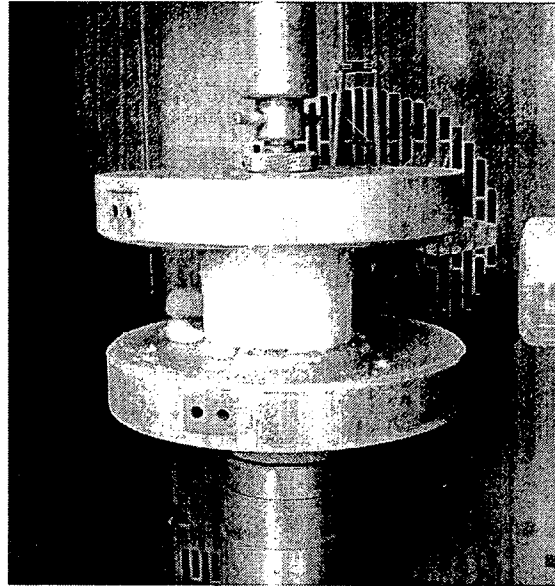


**Fig. 15.** Unconfined compression test

The load cell used had a capacity of 10 kN, with a resolution of  $\pm 0.5\%$  down to 200 N, and  $\pm 1\%$  down to 100 N.

### 3.2.3 Test parameters

Tests were carried out with the parameters varied as shown in Table 5. The aspect ratios are noted here for reference only. Cylinder height and diameter were the controlled variables.

**Table 5.** Unconfined compression testing parameters

Parameter	Values tested	Units
Cylinder diameter	27, 33, 47, 64	mm
Cylinder height	10, 26, 38, 44	mm
Cylinder aspect ratio	0.16, 0.21, 0.30, 0.37, 0.41, 0.55, 0.59, 0.69, 0.79, 0.81, 0.94, 0.96, 1.15, 1.33, 1.41, 1.63	
Compression amount	90% of cylinder height, or until the load cell hit its safety stop	
Compression speed	5	mm s <sup>-1</sup>
Snow average grain size	1	mm
Load cell used for test	10 kN capacity with resolution +/-1%	

The ductile-to-brittle transition normal strain rate for snow is about  $10^{-4} \text{ s}^{-1}$  (Kirchner, Michot, and others, 2001). Strain rates for this set of testing were selected to be well above this number, but also low enough to minimize inertial effects.

In total, 6 runs of each diameter and height combination were tested. Of these 96 data points, about 80-90 were usable for each data report. Not all tests provided all data points because some data points required certain geometric criteria to be met, and some geometries were outside of these ranges.

### 3.3 Results

#### 3.3.1 Characterization of snows

It was determined that the type of snow that occurs with high regularity in aged snow packs in Fairbanks has medium rounded grains, as described in the ICSSG (Fierz and others, 2009). Snow densities measured ranged from 150 to 170 kg/m<sup>3</sup>, and the average grain size was less than 1 mm. Texture index, which is an empirical number defined by the ratio of mean grain

size in mm to density in  $\text{kg/m}^3$ , ranged from 3 to 4.5. Observations and measurements were similar for three consecutive winters, 2008-2009, 2009-2010, and 2010-2011, such that test results from snows of different winters are deemed to be comparable.

### 3.3.2 Failure modes

Four failure modes were observed.

- (i) The first, which occurred for most of the mid-range aspect ratios, was that the cylinder would compress cleanly for the first few millimeters, and then the cylinder would abruptly crumble into a roughly conical pile. The pile would then compress until the test arrested itself due to reaching either the programmed 90% compression, or the load cell's limit. After the test, the compressed pile would be observed to be mostly unsintered snow, which would slide or brush easily off the platen.
- (ii) The second, which occurred for the smaller aspect ratios, was that the cylinder would compress cleanly throughout the entire test, forming a dense puck. After the test, the puck would be observed to be strongly sintered, but it would not be adhered to the platen.
- (iii) The third, which occurred for only three of the mid-range aspect ratios, was that the cylinder would begin to compress cleanly, but then it would fracture into two vertical pieces. Then the compression would continue as in mode (i), and the two columns would compress slightly further until the snow crumbled into a roughly conical pile and proceeded as in mode (i).

- (iv) The fourth are the tests that aborted, and whose data were not used. For aspect ratios greater than 1.4, the columns were unstable and capsized before the test could yield good results. These tests were aborted, and data was not taken. Because these tests with high aspect ratios were aborted, buckling was not a factor in any of the tests.

**Table 6.** Failure modes of different aspect ratios

	<u>10 mm height</u>	<u>26 mm height</u>	<u>38 mm height</u>	<u>44 mm height</u>
<u>27 mm diameter</u>	0.37 (ii)	0.96 (i)	1.41 (iv; aborted)	1.63 (iv; aborted)
<u>33 mm diameter</u>	0.30 (ii)	0.79; 1 of (iii), 5 of (i)	1.15; 1 of (iii), 5 of (i)	1.33 (i)
<u>47 mm diameter</u>	0.21 (ii)	0.55 (ii)	0.81 (i)	0.94; 1 of (iii), 5 of (i)
<u>64 mm diameter</u>	0.16 (ii)	0.41 (ii)	0.59 (i)	0.69 (i)

In all four modes, only a little of the snow was observed to stick very slightly to the platens. The boundary conditions between snow and platens may probably be safely described as slipping (non-sticking).

The differences observed between modes (i) and (ii) may not be directly due to aspect ratio. Snow samples are sintered due to the exposure to the warmer air coming from the environment. For a cylinder, aspect ratios that are extreme in either direction ( $\ll 1$  or  $\gg 1$ ), have larger surface area to volume ratios, and thus would lead to faster and stronger sintering. Therefore, the cylinders with the smallest aspect ratios would resist breakage. At the other

extreme, the cylinders with the highest aspect ratios should also resist breakage. However, they could not balance themselves due to buckling, so the observation could not be made.

### 3.3.3 Pressure-displacement curves

Unconfined compression tests were performed six times each, on snow plugs of four different diameters and four different heights, resulting in a range of aspect ratios. For sufficiently high aspect ratios, the pressure vs. displacement curves showed three distinct regions, as shown in Fig. 16, which shows the set of curves for the snow plugs of 47 mm diameter and 44 mm height.

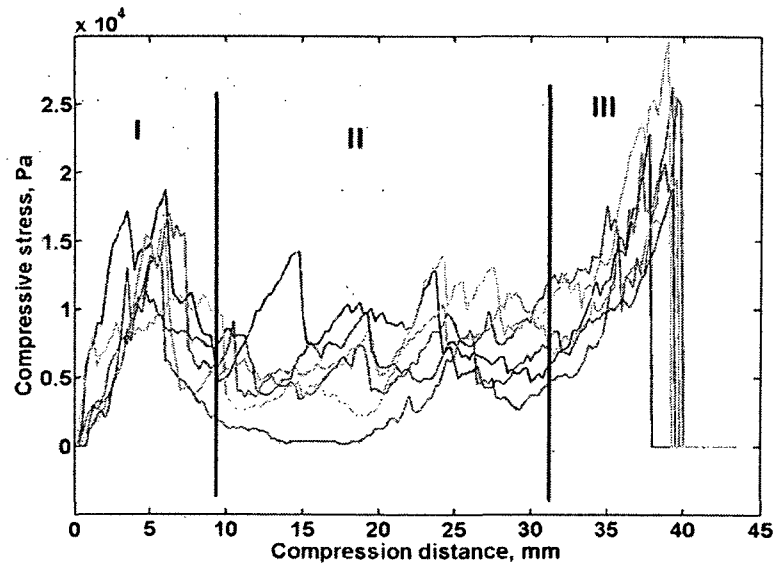


**Fig. 16.** Unconfined compression of 47x44h cylinders of sintered snow, stress versus displacement

Region I shows the snow strength increasing to an initial maximum. Region II is a plateau region, during which the snow strength remains essentially constant as the densification



proceeds vertically throughout the plug. When the compression reaches Region III, the snow is approaching its maximum allowable compression (critical density), so the stress climbs.

The first peak strength captures some of the transient properties of the surface snow, while the plateau value should give a more fundamental value of snow strength. The slope of the stress/compression curve in Region II depends also on the material of the substrate under the snow, so it is not considered as a fundamental descriptor of snow.

For lower aspect ratios, the curves did not display all three regions. For example, Fig. 17 shows the set of curves for the snow plugs of 64 mm diameter and 10 mm height.

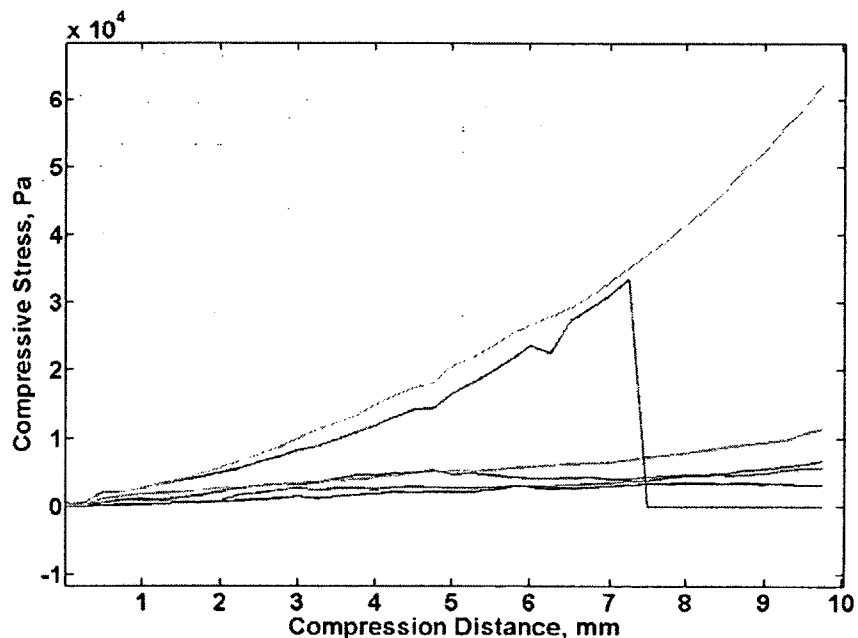


Fig. 17. Unconfined compression of 64x10h cylinders of sintered snow, stress versus displacement

In this set of tests, only a limited range of aspect ratios could yield a plateau value in the test, since at too high aspect ratios, the snow columns would be unstable and would capsize,

and at too low aspect ratios, critical density was approached before Region II could be reached.

Results are tabulated in the following sections.

### 3.3.4 First peak strength

First peak strengths are shown plotted over snow plug aspect ratio in Fig. 18.

First peak strength has unclear relationships with diameter, height, volume, and surface area, but increases with increasing aspect ratio.

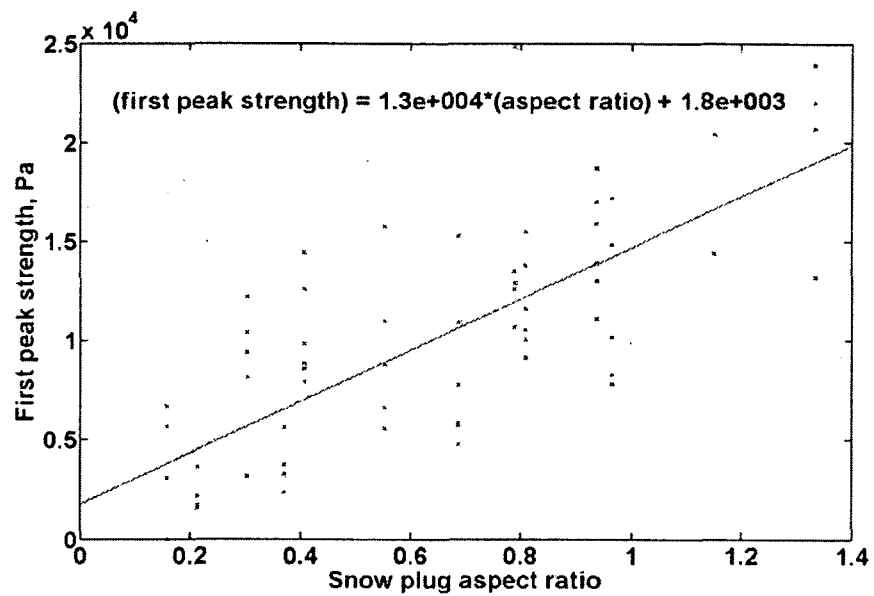
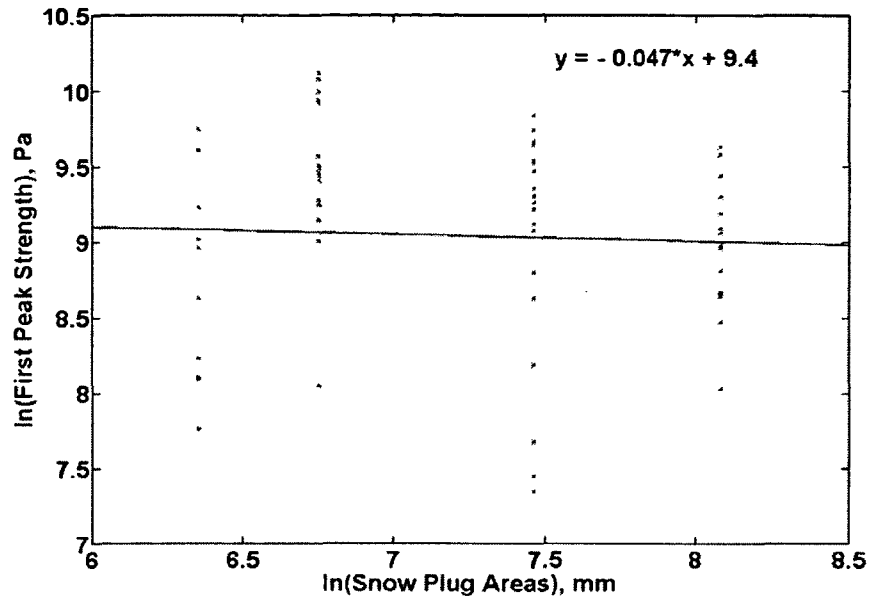


Fig. 18. First peak strength versus aspect ratio

The relationship between first peak strength and cross-sectional area is also tenuous.

However, for purposes of comparison with the indentation data, we have plotted the data shown in Fig. 19.



**Fig. 19.** First peak strength versus cross-sectional area

The exponent is -0.047; whereas for indentation it is 0.83 (Huang and Lee, 2013). Size effects with cross-sectional area are therefore mild with unconfined compression. This means that the goal of unconfined compression testing—to eliminate edge effects—has indeed been achieved. The more solid relationships of properties are with the aspect ratio, which observably affects both the failure strength and mechanism.

### 3.3.5 Plateau strength

Plateau strengths are shown plotted over snow plug aspect ratio in Fig. 20.

Most of the plateau strength values were determined "semi-automatically", similar to the procedure used in (Huang and Lee, 2013), by criteria that were based on the specific test run. The plateau was defined as "When the moving average of X points changes by more than Y

and remains stable for Z data points, then Z is called the plateau." X, Y, and Z were manually selected on a test-by-test basis, due to the large test-to-test variation. A quarter of the resulting plateau strengths came out completely inappropriately, plateau ranges in those cases were hand-selected using careful visual judgment.

Like first peak strength, plateau strength has unclear relationships with diameter, height, volume, and surface area, but increases with increasing aspect ratio.

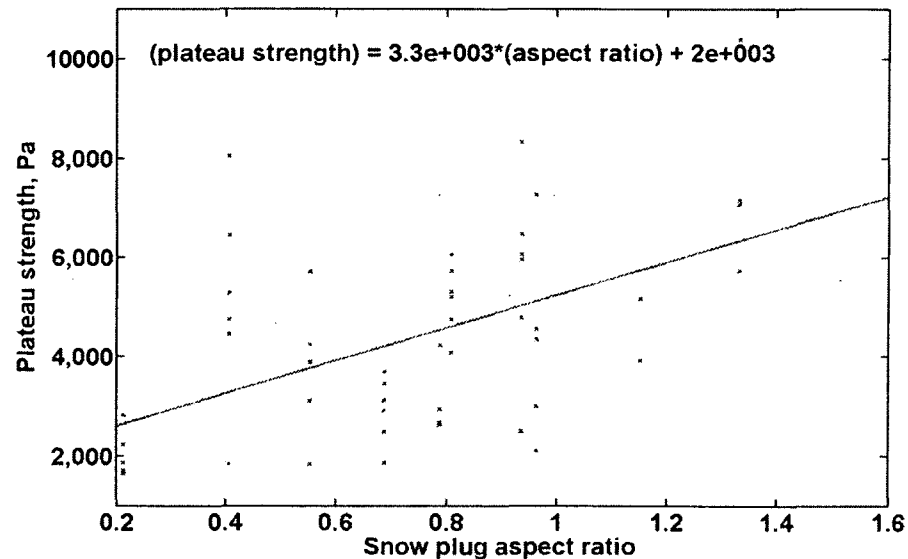


Fig. 20. Plateau strength versus aspect ratio

Plateau strengths are slightly lower, but on the same order of magnitude, as those for indentation tests. When plotted together, as shown in Fig. 21, the pattern shown with indentation—that the compression strength becomes constant at larger diameters—is reflected in the compression data. Indeed, it shows that we may regard unconfined compression as indentation with infinite diameter.

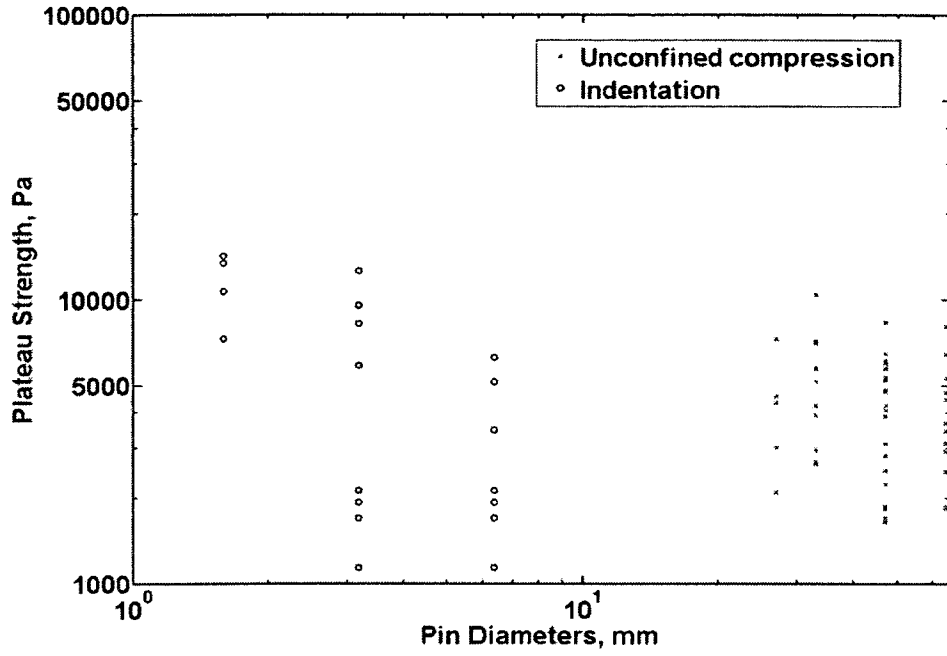


Fig. 21. Plateau strengths of indentation and compression data

3.3.6 Absorption of energy

Energy absorption for each unconfined compression test, from first contact with the snow to the completion of the test (which was set to be 90% the height of each snow plug), is calculated by taking the area under the force-displacement curve, similar to the procedure used in (Huang and Lee, 2013). To normalize against geometric factors and arrive at a dimensionless number, the volumetric density of absorbed energy is calculated by dividing the absorbed energy by the volume of snow displaced and by the Young's Modulus of ice, for which this study uses 9 GPa (Schulson, 1999).

$$\text{Total energy absorbed} = \text{Area under Force-Displacement curve}$$

Volumetric energy density = (Total energy absorbed)/((Volume of snow displaced by the platten)\*(Young's modulus of bulk material))

The results, shown by diameter and by aspect ratio and in Fig. 22 and Fig. 23, respectively, suggest that energy absorption increases with increasing aspect ratio, while the relationships with diameter, height, volume, and surface area are unclear.

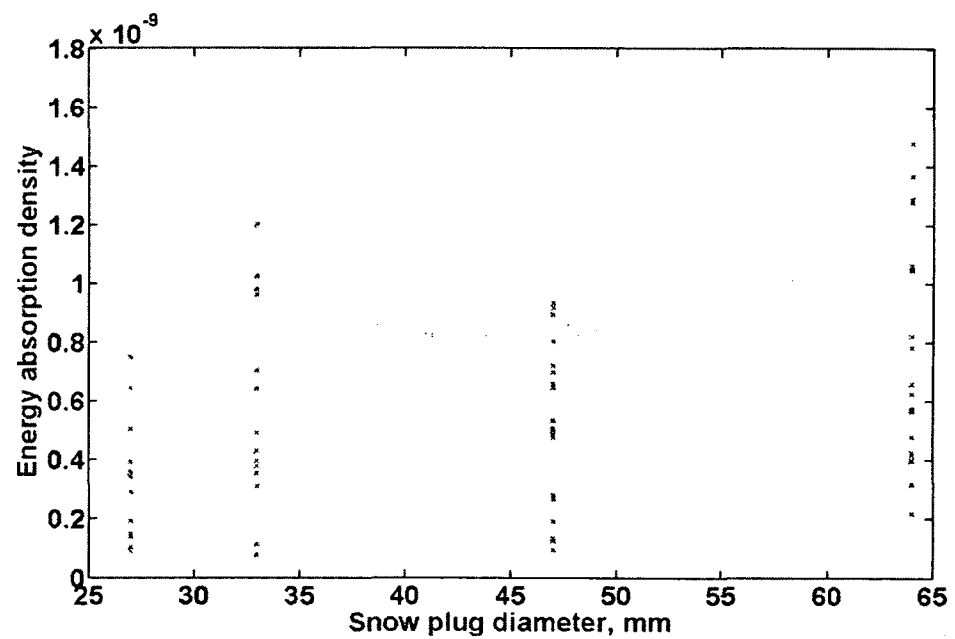


Fig. 22. Energy absorption versus diameter

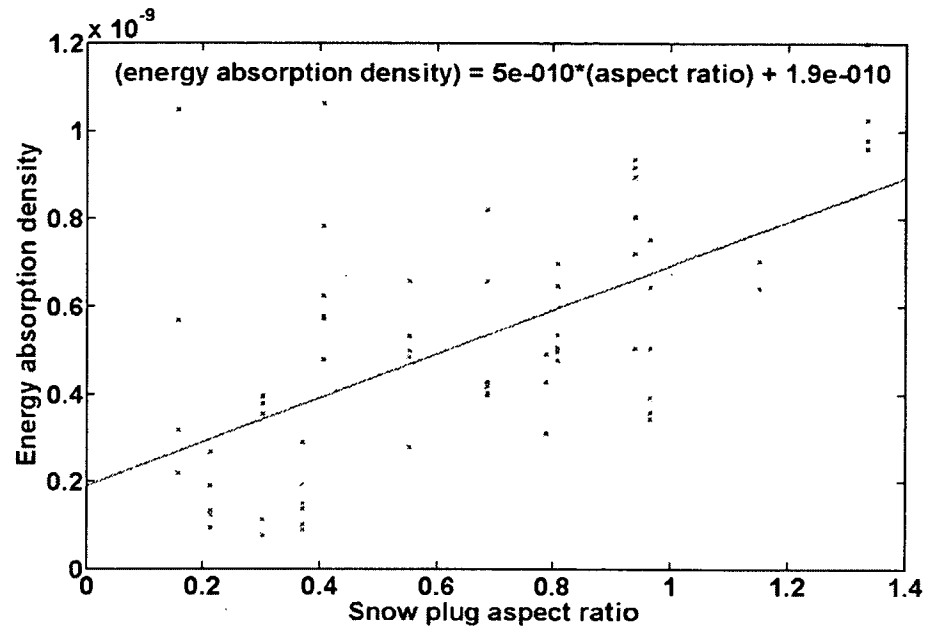


Fig. 23. Energy absorption versus aspect ratio

Energy absorption is about three orders of magnitude lower than for indentation. This indicates that the confining pressure of the surrounding snow during indentation is significant.

### 3.4 Discussion

#### 3.4.1 Overall test observations

It must be noted that this testing all took place with sintered snow, so the material properties will be slightly different from results obtained from unsintered snow. Unfortunately, it is not possible to obtain unconfined compression results from unsintered snow as without a confinement pressure, the only way to do unconfined testing is by sintering the snow into its required geometry.

The biggest differences in results would be expected with the first peak strength, because after the platen makes contact with the snow, it disintegrates within a few mm of displacement. Therefore, the first peak should capture most of the difference between the strength of sintered versus the strength of unsintered snow. However, a comparison between first peak indentation data for sintered versus unsintered snow shows only minor differences, as shown in Fig. 24 vs. Fig. 25.

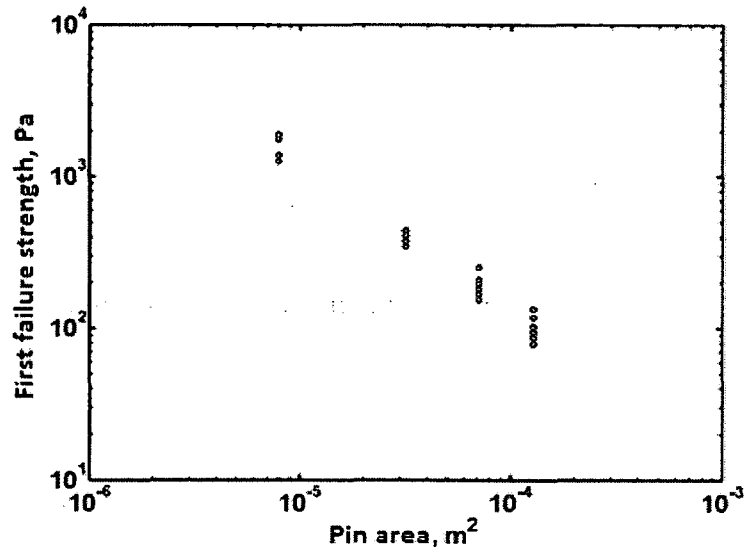


Fig. 24. First peak strength versus pin area, unsintered snow



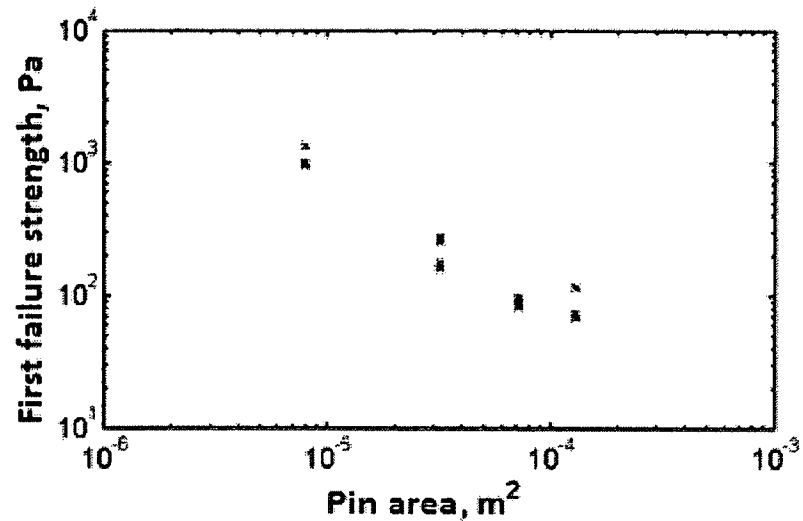


Fig. 25. First peak strength versus pin area, sintered snow

Therefore, this data is presented as comparable to the results from other studies on fresh, virgin snows.

#### 3.4.2 Discussion of results

Both first peak and plateau strengths decrease slightly with increasing diameter, but increase strongly, linearly, and generally monotonically with increasing aspect ratio before buckling has occurred. This suggests that snow mechanical behavior in unconfined compression is more strongly dependent on aspect ratio than on diameter. This seems reasonable, as without edge effects, the diameter of the snow seems relevant only in relation to other metrics, which in this case is snow plug height.

A higher aspect ratio means that for the same snow plug height, the smaller diameter will display greater strength than the larger diameter. This is consistent with the indentation test results (Huang and Lee, 2013). It also means that for the same snow plug diameter, the higher

snow plug height will display greater strength than the lower height. The mechanisms behind this are not understood.

The plateau strengths are reflective of the plateau strengths obtained from indentation testing, with the unconfined compression testing representing an indentation with a “pin” of infinite size.

Energy absorption density increases slightly with increasing diameter, and increases strongly, linearly, and generally monotonically with increasing aspect ratio. The mechanisms behind this are not understood either.

### **3.5 Conclusions**

In nature, snow is subjected to many external forces and environmental factors, such as wind, impurities, temperature fluctuations, and humidity. All of these factors affect snow behavior. This study attempted to remove all of those factors and obtain properties of “pure” snow on a fundamental level. However, as the results are applied to other work, the external factors will need to be taken into account as they affect snow’s intrinsic strength and its surface properties. The snow tested was also sintered slightly, but unaltered in any other way before testing. This is a situation that does occur in nature, but not under such highly controlled conditions. Because only enough sintering was allowed for the testing to take place, results of this study should be considered more comparable to those of unsintered snow, instead of fully sintered snow, which is capable of bearing much higher loads.

Additionally, properties of any materials that interface with the snow will need to be taken into account along with the properties of the snow.

It must also be noted that the size effects discussed in this paper have only been tested on the scales reported, and should not be extrapolated beyond the end points of the data presented here.

The key conclusions from this study are:

- 1) Both first peak and plateau strengths decrease slightly with increasing diameter, but increase strongly, linearly, and generally monotonically with increasing aspect ratio.
- 2) Energy absorption density increases slightly with increasing diameter, and increases strongly, linearly, and generally monotonically with increasing aspect ratio.

#### **Acknowledgements**

We gratefully acknowledge support for this work by the U.S. Army TACOM Life Cycle Command under Contract No. W56HZV-08-C-0236, through a subcontract with Mississippi State University. This work was performed in part for the Simulation Based Reliability and Safety (SimBRS) research program. Any opinions, findings and conclusions or recommendations expressed in this material are those of the authors and do not necessarily reflect the views of the U.S. Army TACOM.

Disclaimer: Reference herein to any specific commercial company, product, process, or service by trade name, trademark, manufacturer, or otherwise, does not necessarily constitute or imply its endorsement, recommendation, or favoring by the United States Government or the Department of the Army (DoA). The opinions of the authors expressed herein do not necessarily

state or reflect those of the United States government or the DoA, and shall not be used for advertising or product endorsement purposes.

## References

- Bazant, Z.P. and Y. Xiang 1997. Size effect in compression fracture: splitting crack band propagation. *ASCE Journal of Engineering Mechanics*, 123: 161-172.
- Edens, M.Q. and R.L. Brown 1991. Changes in Microstructure of Snow under Large Deformations. *Journal of Glaciology*, 37(126): 193-202.
- Fierz, C., R.L. Armstrong, Y. Durand, P. Etchevers, E. Greene, D.M. McClung, K. Nishimura, P.K.S. Satyawali and S.A. Sokratov 2009. *The International classification for seasonal snow on the ground*. Technical documents in Hydrology, 83: 90 p.
- Fukue, M. 1979. Mechanical Performance of Snow Under Loading. Tokai University Press.
- Huang, D. and J.H. Lee 2013. Mechanical properties of snow using indentation tests: size effects. *Journal of Glaciology*, 59(213).
- Jellinek, H.H.G. 1957. Compressive strength properties of snow. *Journal of Glaciology*, 3(25): 345-354.
- Kirchner, H.O.K., G. Michot, H. Narita and T. Suzuki 2001. Snow as a foam of ice: Plasticity, fracture and the brittle-to-ductile transition. *Philosophical Magazine A*, 81(9): 2161 - 2181
- Lang, R. and W. Harrison 1995. Triaxial tests on dry, naturally occurring snow. *Cold Regions Science and Technology*, 23(2): 191-199.
- Lee, J.H. 2011. An improved slip-based model for tire-snow interaction. *SAE International Journal of Materials and Manufacturing*, 4(1): 278-288.
- Schulson, E.M. 1999. The structure and mechanical behavior of ice. *Journal of the Minerals Metals & Materials Society*, 51(2): 21-27.

- Shoop, S.A. and R. Alger 1998. Snow Deformation Beneath a Vertically Loaded Plate: Formation of Pressure Bulb with Limited Lateral Displacement. *Proceedings, ASCE Cold Regions Specialty Conference*.
- Tang, CA , Wong, RHC., Chau, KT and Lin, P 2005. Modeling of compression-induced splitting failure in heterogeneous brittle porous solids. *Engineering Fracture Mechanics*, 72: 597-615.
- Wong, J.Y. 2001. *Theory of Ground Vehicles*. 3rd ed. Wiley, New York
- Yong, R.N. and M. Fukue 1977. Performance of Snow in Confined Compression. *Journal of Terramechanics*, 14(2): 59-82

#### 4 Mechanical properties of snow using cone penetration tests: size effects <sup>3</sup>

Daisy HUANG, Jonah H. LEE

Keywords: Snow, snow indentation, snow penetration, cone penetration, Snow Penetrometer, Snow MicroPenetrometer, SMP, Size Effect

**ABSTRACT.** Behavioral models of snow, a naturally-occurring, heterogeneous material, are useful to both natural scientists and engineers, who are interested in the interactions between ground vehicles and terrain. Snow's microstructure, and therefore its behavior, depends on thermal and mechanical history, as well as on current conditions (e.g., temperature and moisture content). This study examines the correlation between snow's current microstructure and its mechanical behavior under cone penetration testing, which is commonly used by geologists and avalanche researchers to characterize the properties of soils and snows. For random heterogeneous materials, it is known that the response of a penetrometer should depend on the size and geometry of the penetrometer tip relative to that of the snow microstructure, although this effect has not been systematically studied. This study mimics the cone tip geometry from a standard penetrometer, and uses it on natural snows under controlled laboratory conditions. The size and included angle of the cones used in the laboratory testing were varied, and the results compared against both in situ snow testing using a standard snow penetrometer and theoretical expectations. It was found that empirical values of snow strength may be obtained from the testing. Size effects are also apparent—the larger the cone tip diameter and the larger the cone angle, the higher the apparent strength.

---

<sup>3</sup> Huang, D. and J.H. Lee, prepared for submission in Cold Regions Science and Technology

#### 4.1 Introduction

A comprehensive study of ground-vehicle interaction requires a quantitative description of the ground's response to load. In regions with cold, snowy winters, the ground itself remains frozen, and the mechanical properties of the snowy cover dominate the mechanics of the of the ground-vehicle interaction. The mechanical properties of snow depend on microstructure, which is a function of both thermal and loading history, and the current physical environment, i.e., air temperature and humidity. Instead of quantifying material properties as functions of all of these independent variables, it is more useful and practical to quantify material properties as functions of the current state (microstructure, density, and temperature) of the snow, regardless of how it got there. Therefore, it is useful to define certain snow mechanical properties that are measurable and yield an accurate model and description of the snow.

The Snow MicroPenetrometer (SMP), developed by Schneebeli and Johnson (1998), and introduced by Schneebeli, Pielmeier, and Johnson (Schneebeli, Pielmeier et al. 1999), of the Swiss Institute for Snow and Avalanche Research, is one method to measure a snowpack's mechanical and microstructural properties. The SMP consists of cone tip containing a load cell, mounted on a rod that moves in a linear motion and drives a cone tip into the snow under examination. The load cell on the cone tip reads the instantaneous resistance force of the snow as the cone penetrates the snow layers.

The cone tip is sufficiently sharp to capture individual ruptures of snow crystal bonds. The SMP outputs the signal of force vs. penetration distance, and when this is correlated against the penetration speed, it can give information about average grain size and snow strength. A detailed analysis of how the data output is analyzed is given in Johnson (2000).



The SMP has been used to evaluate natural snow-packs as well as to study how a snowy terrain is altered after vehicle traversal. Conical penetration into snow has also been modeled with simulations (Lee, Huang et al. 2011).

In this study, the cone penetration test was reproduced in a controlled laboratory environment. The cone tip was varied in angle and diameter. Because size effects have been observed in flat pin indentation testing (Huang and Lee 2013), analogous size effects were sought for cone penetration testing.

Natural snows, selected for consistency in density and microstructure, were collected and brought into the laboratory for storage and testing. The Snow MicroPenetrometer was used at the snow collection sites, and base values were obtained for snow strength. Then, analogous cone tips were machined, which varied in diameter and included angle. The same testing methodologies were used for all of the different cone geometries, and the effects of snow cone geometry on apparent snow strength were tabulated and studied. Flat-tipped cylindrical indenters (included angle of 180 degrees) were also tested and used for comparison (Huang and Lee 2010), (Huang and Lee 2013).

## **4.2 Background**

### **4.2.1 Prior work**

Various types of cone penetrometer have been used by geologists and avalanche researchers to characterize different types of ground covers, e.g., soils, sands, and snows. Historically, the most common type of penetrometer used for snow was a rammsonde, which is a ram penetrometer with a cone face area on the order of 10s of  $\text{cm}^2$  (Haefeli 1939; Mellor

1974; Perla and Martinelli 2004). It is used by dropping a weight onto the back of the cone, and gives a measurement of the strength of the cumulative snowpack. A smaller penetrometer that reads resistive force while being pushed by hand into the snow was developed by Mackenzie and Payten (2002). Later, methods were developed to measure the snow resistive force during penetration at a controlled speed. Dowd and Brown (1986) developed an instrument called a Digital Thermal Resistograph, which during penetration used strain gages and a microprocessor to record a data point every millimeter. The area of the leading face was  $5 \text{ cm}^2$ . Another electric cone penetrometer was developed by Schaap and Föhn (1986). McCallum, Barwise, and Santos (2010, 2011) observed that prior snow penetrometer work was limited in depth and capacity, and developed and tested a very large scale penetrometer with a capacity of 10 kN, a stroke of 70 cm, and a potential to record snow strength to a depth of 5-10 m.

Johnson and Schneebeli (1999) pushed the boundary of knowledge in the opposite direction by using a micropenetrometer of tip area  $20 \text{ mm}^2$ . They used a micromechanical theory of penetration to invert the force-distance signal from the Snow MicroPenetrometer to estimate the mechanical properties of a given snow pack. Their algorithm uses a Monte Carlo simulation of snow properties over a range of possible values for the snow's mechanical parameters. When this algorithm is applied to a force-distance signal, such as is output from the SMP, the signal may be inverted, and micro-mechanical strength may be estimated. From the output of the SMP, the macro-mechanical strength may then also be calculated from other output parameters.

This statistical treatment of the mechanics of snow was later expanded and generalized to form a micromechanical theory of cone penetration in granular materials in general (Johnson 2003).

#### 4.2.2 Cone penetration theory

The Snow MicroPenetrometer used was developed by Johnson and Schneebeli (1999) for use in avalanche research. The raw output of the Snow MicroPenetrometer is penetration force and texture index as a function of penetration depth. Texture index is an empirical value used to quantify the snow grain geometry. It is defined by the ratio of mean grain size in mm to density in  $\text{kg/m}^3$ .

Micro-mechanical strength refers to strength on small scales (on the order of the size of the snow grains), and it correlates with the strength of individual ice bonds, while macro-mechanical strength refers to strength over larger scales, which account for the bonds' random orientation, and correlates with the strength of the bulk snow. Since any given bond is not generally oriented in its direction of greatest strength, macro-strength is almost always smaller than micro-strength.

The algorithm makes the following assumptions:

- The force measured at the cone tip is comprised of three components, which superpose: friction between the cone tip and the snow, elastic deflection of the snow, and rupture of micro-structural elements in the snow matrix.
- The effects of snow compaction are negligible. Johnson and Schneebeli show that this is a safe assumption for the SMP half angle of 30 degrees.

- The microstructural elements are randomly distributed around a mean constant dimension  $L_n$ .

The second assumption becomes tenuous as the included angle and diameter of the penetration tip increase to where the effects of compaction become significant. The larger the ratio of penetration pin diameter to average snow grain size, the more compaction takes place. Johnson has developed a model that takes compaction into account (Johnson 2003), but it is not accounted for in this algorithm yet.

Results from indentation testing with flat-tipped indenters (Huang and Lee 2013) results have shown that compaction takes place beneath the cylindrical pin tips. To observe that compaction takes place beneath an included half angle of 90 degrees, and that compaction is negligible beneath an included angle of 30 degrees, implies that at some particular angle, compaction becomes important.

The SMP penetration model is statistical in nature and calculates a micro-mechanical strength by taking the product of the average number of intact structural elements in contact with the cone's leading face, and the axial force contribution of each microstructural element. The macro-mechanical strength is then calculated by multiplying the micro-mechanical strength by the probability of contact between the penetrometer tip and a microstructural element.

#### **4.3 Experimental procedures**

Snow falls in many different types, depending on atmospheric and ground conditions (Fierz, Armstrong et al. 2009). However, in the cold, dry, windless conditions of Fairbanks winters, once it lands, it metamorphoses within a few weeks to one of a few stable snow types.

For this study, two different snow types were selected. The first was snow that had fallen a few weeks to a few months prior, which will be called “fine-grained snow”. The other was snow that had fallen over a few months prior, and had been insulated under layers of fresher snow. These conditions lead to growth of larger crystals, called depth hoar. In this paper, this will be called “coarse-grained snow”. These two types were selected because they occur very commonly, so they have the dual advantage of being both easy to find and of having broad applicability, since they are commonly encountered by ground vehicles.

Before collection of snow for laboratory testing, several quick methods were used onsite to characterize the snow. For consistency and purity of data, cold, sheltered areas were selected for testing on cold, dry days. First, a snow pack was selected visually for the desired snow type, and tested in-situ using a high-resolution Snow MicroPenetrometer. Then samples were removed and measured, weighed, and sieved to estimate density and grain size distribution. Finally, specimens were collected, stored in coolers, and brought to the laboratory. There, they were additionally characterized via optical inspection with a light microscope, and CT scanning using 3D X-ray MicroTomography.

After the snows were characterized and determined to be the desired type for testing, they were used in cone penetration testing.

#### 4.3.1 In-situ snow testing, collection, and characterization

The Snow MicroPenetrometer readings, density measurements, weighing and sieving, and CT scanning all established baseline microstructures for different natural snows in their

natural state, using the International Classification for Seasonal Snow on the Ground (Fierz, Armstrong et al. 2009).

#### 4.3.1.1 Snow MicroPenetrometer

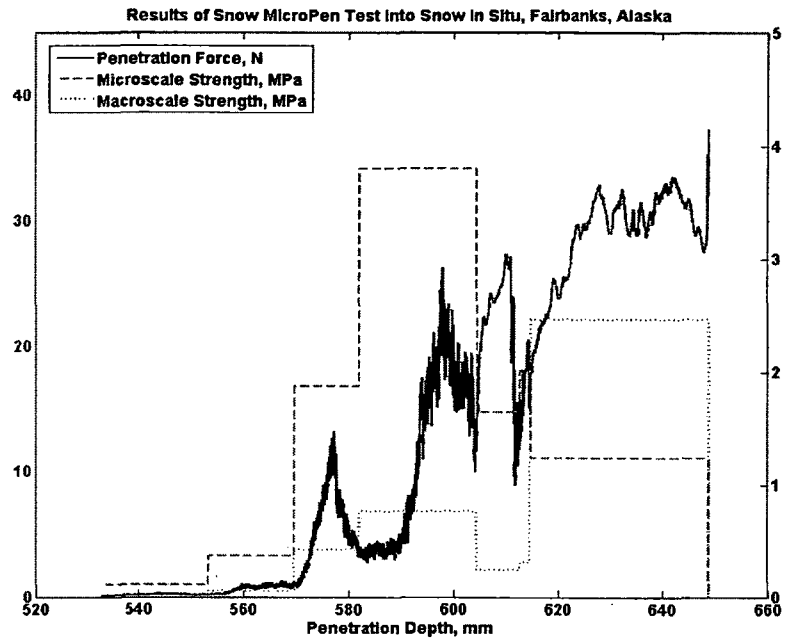
The unmodified Snow MicroPenetrometer was used to test natural snows in the Fairbanks area. Sites were selected that displayed the types of conditions of interest for this study, that is, clean, dry, metamorphically stable snows that were representative of the type that remains on the ground throughout most of a typical winter in Fairbanks. The Snow MicroPenetrometer is brought to the outside temperature, and mounted onto two poles, which have adjustable baskets on them. The SMP is used by adjusting the baskets so that the cone tip is about 6-10 cm above the snow surface, holding the assembly so that penetration occurs in the direction normal to the snow layers, and then allowing the penetration test to proceed. Penetration tests were performed at least 15 cm apart, so that the penetration hole from one test did not affect the next. These procedures, and preliminary results, have previously been reported in Huang and Lee (2011).

Fig. 26 shows the SMP in a sample test environment.



**Fig. 26.** SMP in field test environment

Marshall's algorithm (Marshall and Johnson 2009) was used to invert the force vs. depth signal output and obtain a strength measurement for each snow layer. An example output from one full test, with the results from the algorithm, is shown in Fig. 27.



**Fig. 27.** Example of SMP output for a complete snowpack reading

Because this study concerns itself with snow's interaction with ground vehicles, its focus is on the top few layers of snow, whose mechanical properties have the largest bearing on such interactions. Fig. 28 shows the same data, zoomed in to the layers of interest.



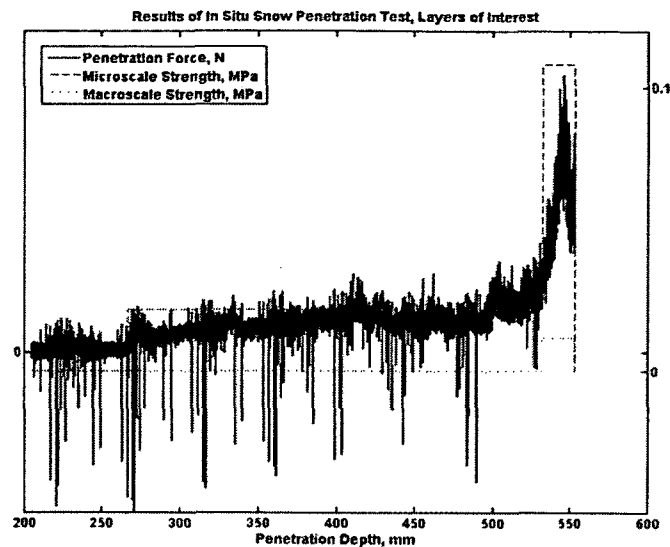


Fig. 28. SMP output, zoomed in to area of interest

#### 4.3.1.2 Other on-site snow characterization tests

Snow density was measured at field collection sites using a graduated cylinder of known mass, hanging from a spring scale. This gave an estimate of density that was later compared against the density obtained from the CT scan images.

Grain size distribution was obtained on-site by sieving, with sieves of 1.4, 1, and 0.425 mm. From this sieving, average grain sizes were estimated to be 1 mm for the fine-grained snow, and 2.2 mm for the coarse-grained snow.

#### 4.3.1.3 Collection and storage of snow

The snows under study were chosen for being commonly occurring and metamorphically-stable. To eliminate effects of moisture and water menisci, snow was only collected on cold days.

Aged (metamorphically quasi-stable), dry, undisturbed snow was collected in and around Fairbanks, Alaska, at temperatures between -9 and -30 degrees C. After sufficient aging has taken place to have metamorphic stability, the crystals are roughly spherical and with a consistent distribution of grain sizes.

Two types of stable snow were collected for testing. The first was fine-grained (average grain size under 1 mm) snow such as occurs near the surface of snow pack. The second was coarse-grained (average grain size over 1.5 mm) depth hoar such as occurs under 20 cm beneath the snow surface. Air temperature, snow surface temperature, and snow pit temperature under the surface were measured and recorded at each snow collection.

Samples were collected in plastic containers and transported to the laboratory freezers in a cooler. Laboratory freezers were maintained at -30° C, which is cold enough to slow metamorphism and sintering to a very low rate (after six months in storage, little sintering had taken place among the snow crystals). Storage time ranged from less than a day to two months.

#### 4.3.1.4 Laboratory testing of snow for confirmation of snow selection

Snow samples were scanned using a CT scanner that was housed in a cold room. Samples were scanned at 23.7- $\mu\text{m}$  resolution using parameters as recommended by H. Yuan (2007). The resulting scans were used to confirm density and average grain size.

At the beginning of testing, a few samples were also examined optically using a light microscope.

#### 4.3.2 Cone penetration testing

A CETR UMT tribometer was selected for testing due to its high-resolution load cell and its ease of adaptation to individual tests. The load cell used had a range of 5 - 500 mN and a resolution of 0.050 mN. It was maintained at a temperature of  $-20^{\circ}\text{C}$  using a low-temperature forced air stream, set to an output of  $-40^{\circ}\text{C}$ . The reason for the temperature difference is that the enclosure has some inevitable leakage due to the necessity of openings for the tribometer interface.

Fig. 29 shows a photo of the cold temperature chamber.

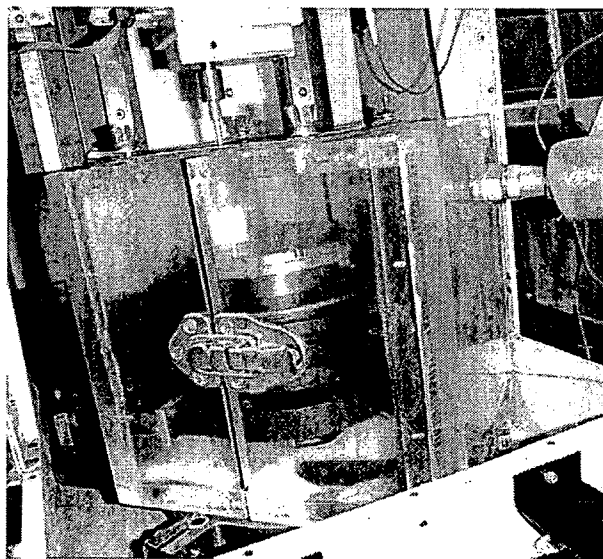


Fig. 29. Cold temperature enclosure

Fig. 30 shows a schematic of the cone penetration laboratory test setup. The top of the cone penetration tip is coupled to the load cell, which reads force in the vertical direction as the penetration is proceeding.

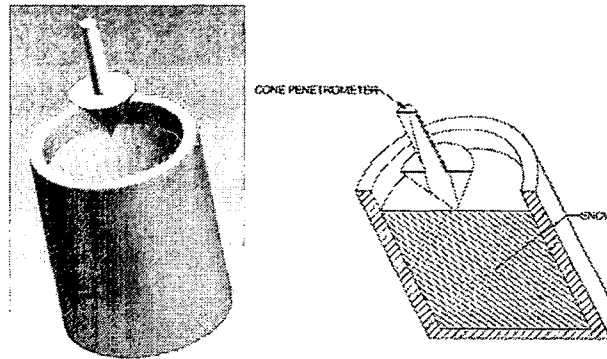


Fig. 30. Schematic of cone penetration test

#### 4.3.2.1 Test parameters

Table 7 shows the parameters that were varied for the laboratory tests. The other factors that were altered, such as the sampling frequency and penetration rate, were not altered by choice, but were altered due to equipment limitations. However, the values are sufficiently close to the Snow MicroPenetrometer values that they should not affect the test results.

The ductile-to-brittle transition strain rate and the transition to linear elastic behavior have been separately reported as approximately  $10^{-4} \text{ s}^{-1}$  (Kirchner, Michot et al. 2001), and  $10^{-3} \text{ s}^{-1}$  (Shapiro, Johnson et al. 1997), respectively. Whatever uncertainties there may be in those reported values, the testing here induces strains at rates on the order of  $10^{-1} \text{ s}^{-1}$  (Marshall and Johnson 2009) two orders of magnitude higher than the higher reported critical value.

**Table 7.** Test parameters

<u>Parameter</u>	<u>Unit</u>	<u>Snow MicroPenetrometer</u>	<u>Cone penetration tests in laboratory</u>
Penetration speed:	mm/s	20	5
Sampling resolution (sampling rate):	Hz (data points/mm)	5000 (250)	2000 (400)
Force resolution on load cell:	N	0.005	0.00005
Cone tip half angle:	degrees	30	15, 30, 45
Cone tip diameter:	mm	5	2.5, 3.0, 4.0

#### 4.4 Results

##### 4.4.1 Characterization of snows

It was determined that the two snow types that occur with high regularity in aged snow packs in Fairbanks are medium rounded grains near the surface (the top 15 to 20 cm), with coarse faceted rounded particles beneath the fine-grained layer, as described in the International Classification for Seasonal Snow on the Ground (Fierz, Armstrong et al. 2009). Snow densities measured ranged from 148 to 251 kg/m<sup>3</sup>, with the fine-grained snow generally ranging from 150 to 170 kg/m<sup>3</sup> and the coarse-grained snow from 200 to 230 kg/m<sup>3</sup>. The fine-grained snow had an average grain size of less than 1 mm, while the coarse-grained snow had an

average grain size of greater than 1.5 mm. Texture index values were found to be around 3-4.5 for fine-grained snow, and around 5-7 for coarse-grained snow. Observations and measurements were similar for three consecutive winters, 2008-2009, 2009-2010, and 2010-2011, enough to instill confidence that test results from snows of different winters are comparable.

#### 4.4.1.1 Characterization of snows from SMP

Twelve SMP tests were made on a cold day (<-15 degrees C) in Fairbanks, following a large snowfall of about 0.5-1 meter overnight. Because the weeks prior to the snowfall had also been quite cold, the rate of metamorphosis of the older snow was low, and the fresh snowfall served to insulate the underlying crystals from subsequent weather changes and thus preserve them from further metamorphosis. The example penetration depicted in Fig. 28 shows data beginning under the top protective layer, in this case at a depth of about 530 mm.

From the twelve SMP tests, 32 data sets were obtained (each test found between 3 and 5 distinct snow layers, and only the data from the layers of interest were used for this study).

Table 8 shows the results.

**Table 8.** SMP In situ results

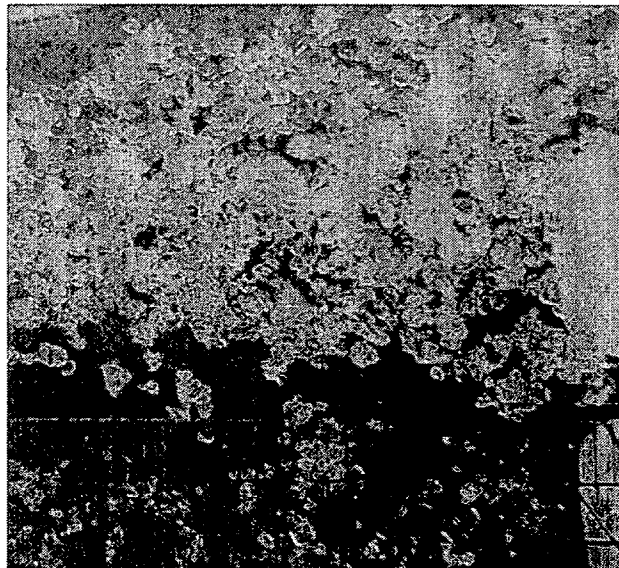
<u>Snow type</u>	<u>Average micro-mechanical strength (MPa)</u>	<u>Average macro-mechanical strength (MPa)</u>
Fine-grained	0.024	0.011
Coarse-grained	0.68	0.089

These results are consistent with expectation from visual examination of the fine- and coarse-grained snow morphology. The larger crystals of depth hoar that comprise the coarse-grained snow contain sharp, defined angles, due to their formation via crystal growth, and these angles impede crystal movement within the snowpack.

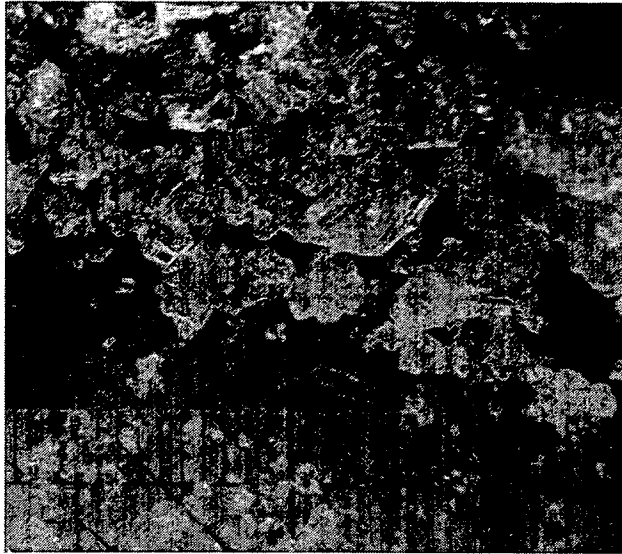
#### 4.4.1.2 Characterization of snows via visual examination

Fig. 31 and Fig. 32 show examples of the fine-grained and coarse-grained snow samples, respectively, that were removed from the layers of interest deduced from the SMP tests and collected for use in the laboratory cone penetration tests.

In Fig. 32, the sharp edges of the snow crystals are clearly visible.



**Fig. 31.** Optical Examination of Fine-Grained Snow



**Fig. 32.** Optical Examination of Coarse-Grained Snow

#### 4.4.2 Laboratory cone penetration results

Micro-scale snow strength, by definition, should be independent of size effects.

However macro-scale snow strength should depend on cone penetration tip size and geometry.

With regards to tip size, the larger the cone diameter, the lower the evident macro-scale strength should be. With regards to the penetration angle, the larger the angle is, the higher the macro-scale strength should appear to be, due to the compaction forces that are not accounted for in the algorithm, as previously discussed.

Thus, apparent macro-scale snow strength should decrease with increasing cone tip diameter, and increase with increasing cone tip angle.

The amount of compaction that takes place also depends on the snow average grain size, or, more accurately, the ratio of cone penetration tip size scale to average snow grain size scale.



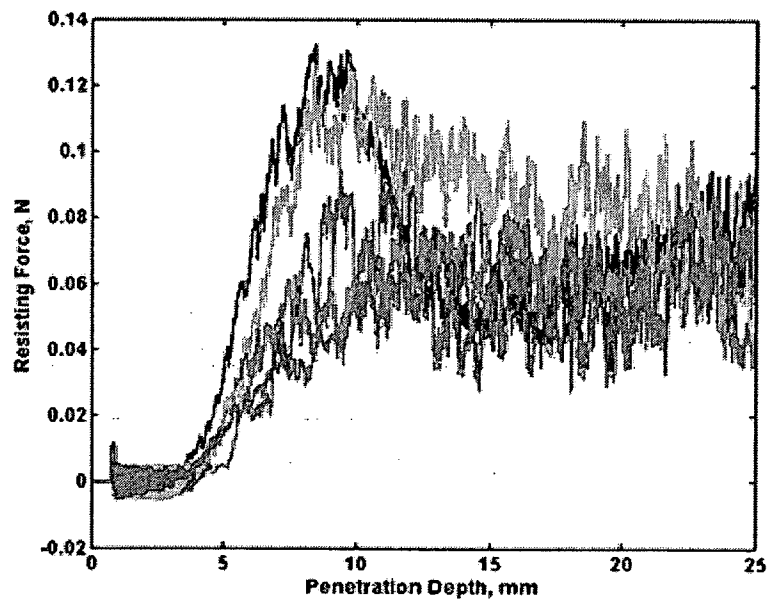
All results are shown in Table 9.

**Table 9.** Snow penetration test results

<u>Snow Type</u>	<u>Cone</u>		<u>Microscopic Strength (MPa)</u>		<u>Macroscopic Strength (MPa)</u>	
	<u>Half Angle (Degrees)</u>	<u>Diameter (mm)</u>	<u>Mean</u>	<u>Coefficient of Variation</u>	<u>Mean</u>	<u>Coefficient of Variation</u>
fine-grained	15	2.5	0.014	0.501	0.007	0.402
fine-grained	15	3	0.024	0.498	0.010	0.466
fine-grained	15	4	0.013	0.456	0.006	0.251
fine-grained	30	2.5	0.021	0.423	0.013	0.460
fine-grained	30	3	0.014	0.360	0.010	0.268
fine-grained	30	4	0.021	0.684	0.011	0.535
fine-grained	45	2.5	0.026	0.326	0.019	0.250
fine-grained	45	3	0.020	0.391	0.015	0.155
fine-grained	45	4	0.012	0.416	0.017	0.492
fine-grained	All fine-grained data		0.018	0.290	0.012	0.357
coarse-grained	15	2.5	0.014	0.471	0.005	0.773
coarse-grained	15	3	0.024	0.491	0.011	0.457
coarse-grained	15	4	0.096	1.923	0.006	0.289
coarse-grained	30	2.5	0.021	0.474	0.012	0.496
coarse-grained	30	3	0.014	0.299	0.010	0.343
coarse-grained	30	4	0.021	0.684	0.011	0.535
coarse-grained	45	2.5	0.022	0.223	0.017	0.225
coarse-grained	45	3	0.018	0.375	0.013	0.305
coarse-grained	45	4	0.010	0.385	0.013	0.583
coarse-grained	All coarse-grained data		0.027	0.993	0.011	0.333

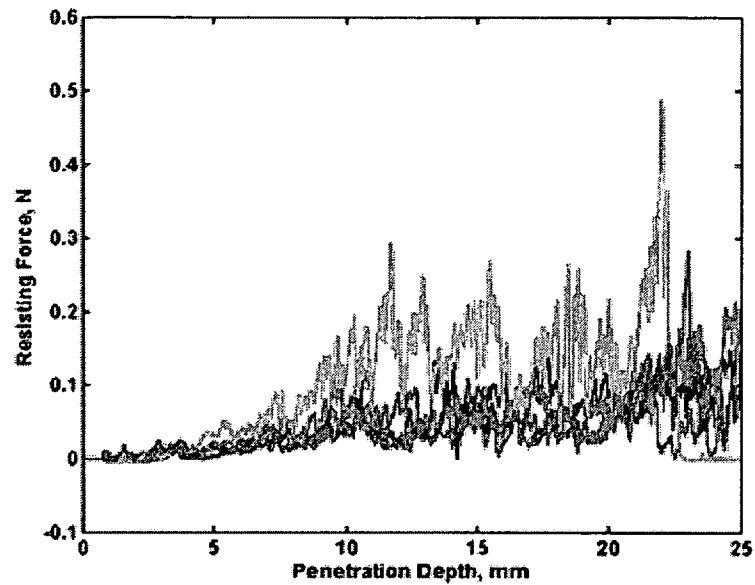
#### 4.4.2.1 Effects of snow grain size

Fig. 33 and Fig. 34 depict a set of force-displacement curves from the laboratory penetration tests using fine- and coarse-grained snow, respectively. Both sets of data depict penetrations of a cone of half-angle 30 degrees and diameter 3.0 mm.



**Fig. 33.** Force-depth data for 30-degree, 3.0-mm cone penetration into fine-grained snow

In the tests using fine-grained snow, some compaction takes place initially, but then the forces level off, implying that no further compaction takes place as the cone drills farther down. In this initial region, a zone of compaction accumulates around the cone tip surface. Once this surface has accumulated, it proceeds downward into the snow along with the cone tip, which Johnson calls the “penetrometer effective surface”. This zone correlates with Zone I in a flat-pin indentation test (Huang and Lee 2013).



**Fig. 34.** Force-depth data for 30-degree, 3.0-mm cone penetration into coarse-grained snow

In the tests using coarse-grained snow, little compaction takes place, because the ratio of penetration cone tip size to average snow grain size is much smaller.

#### 4.4.2.2 Effects of varying cone angle

An example of a set of force-displacement curves for the cone penetration data, with only the angle varying, is shown in Fig. 35 and Fig. 36. Along with Fig. 33, they depict penetration tests of three different cone angles into fine-grained snow with a 3.0-mm diameter cone tip. As the cone angle varies, the average resistance force varies also.

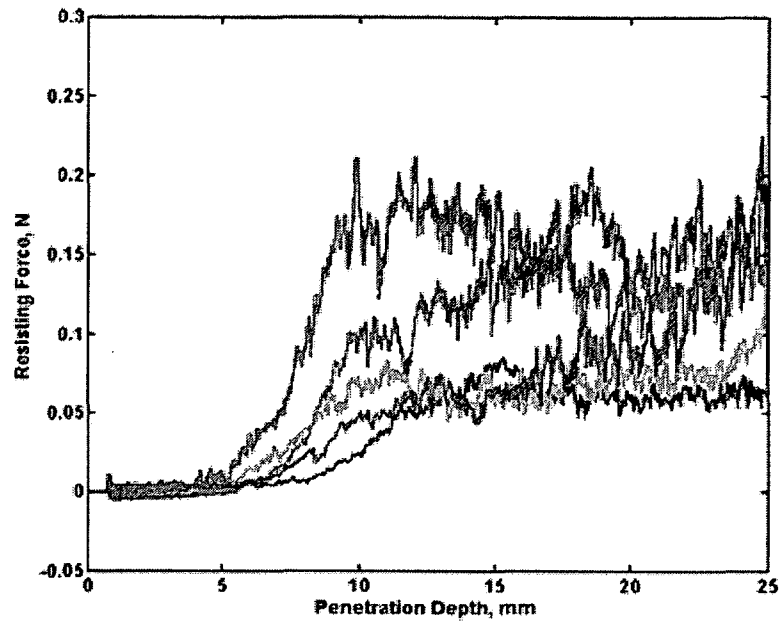


Fig. 35. Force-depth data for 15-degree, 3.0-mm cone penetration into fine-grained snow

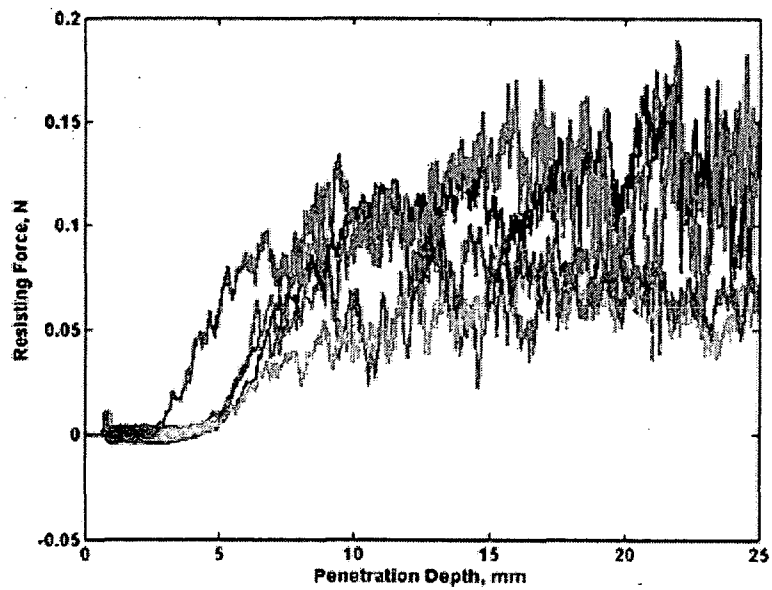


Fig. 36. Force-depth data for 45-degree, 3.0-mm cone penetration into fine-grained snow

The complete results for varying cone angle are displayed in Fig. 37.

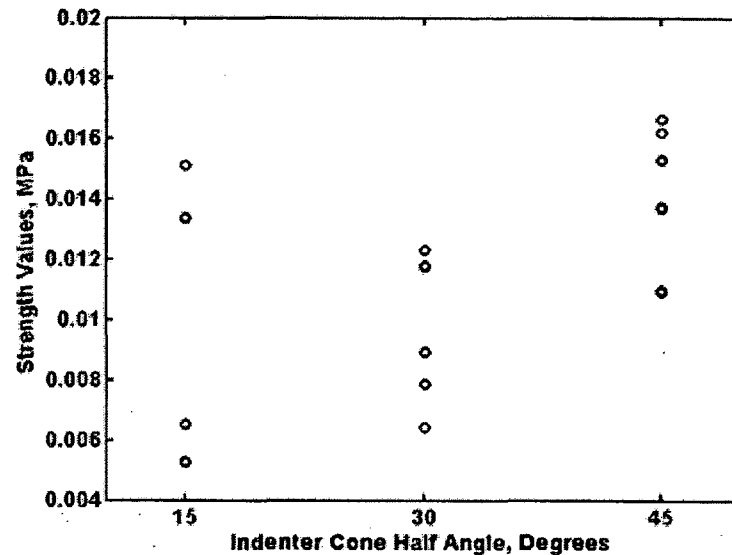


Fig. 37. Macromechanical Strength vs. Cone Angle

The four points in the 0.013 – 0.015 MPa-range for the 15-degree cone tip may be outliers with some systemic cause. We do not have enough data to state this unequivocally, but if they are indeed outliers, then the relationship between penetration angle and apparent macromechanical strength is clear.

#### 4.4.2.3 Effects of varying cone diameter in laboratory cone penetration

An example of a set of force-displacement curves for the cone penetration data, with only the diameter varying, is shown in Fig. 38 and Fig. 39. Along with Fig. 33, they depict penetration tests with three different cone tip diameters into fine-grained snow with a 30-degree half angle cone tip. As the diameter varies, the average resistance force varies also.

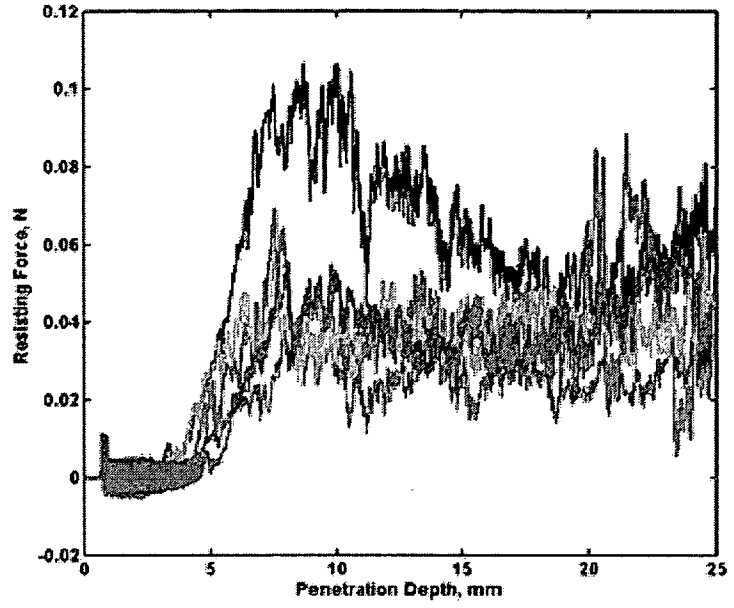


Fig. 38. Force-depth data for 30-degree, 2.5-mm cone penetration into fine-grained snow

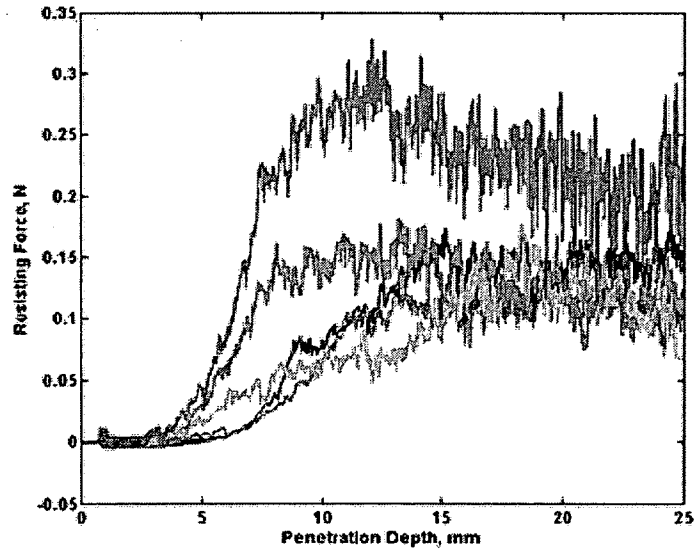


Fig. 39. Force-depth data for 30-degree, 4.0-mm cone penetration into fine-grained snow

The complete results for varying cone diameter are displayed in Fig. 40.

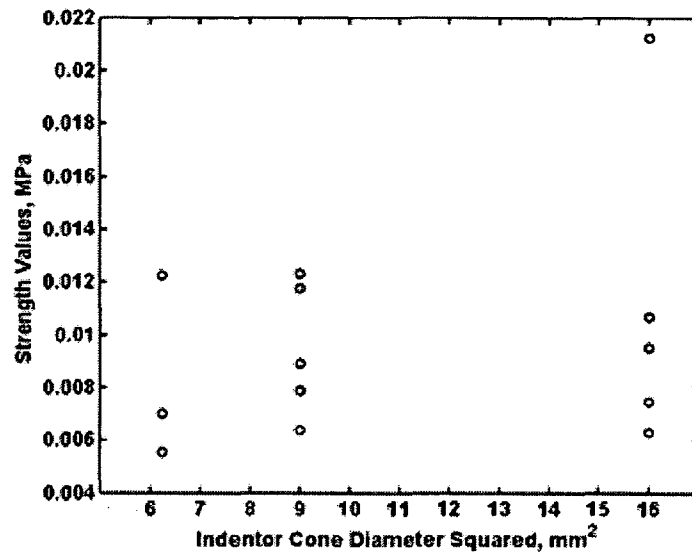


Fig. 40. Macromechanical Strength vs. Diameter Squared

The two points in the 0.02 MPa range for the 4-mm diameter cone tip may be outliers. Without them, the trend of larger cone diameters correlating to lower snow micromechanical strength becomes clearer. This was shown in 2010 with flat-pin indentation tests into snow (Huang and Lee 2013).

#### 4.5 Discussion

The results from the cone penetration data do give a measure of strength that is repeatable and consistent with expectation. However, the calculated macromechanical strength cannot be independently verified on the same sample. Therefore, it is probably safest (most conservative) to regard these strength values as empirical in nature. That is, they may be

regarded as indices of snow strength that will require independent verification before being input into a complete model for snow behavior.

The assumption of negligible snow compaction is the most tenuous, as compaction was both observed in our testing and by other researchers who have done cone penetration testing (LeBaron, Miller et al. 2012). However, if we choose to treat the calculated strength values as empirical, then not accounting for the effects of compaction, which are repeatable and consistent, introduces only a systemic "error" that may not cause problems. Finally, the assumption of negligible snow compaction may indeed be safe, if the Penetrometer Effective Surface remains stiff and propagates through the snow right along with the penetrometer tip itself.

Work has been done with flat-ended cone penetration tests into aluminum foams (Ramamurty and Kumaran 2004). That study, led by U. Ramamurty, considered the compaction of the foam that occurs beneath the flat tip of the cone, taking into account the energy absorbed during formation of the densification zone. It would be interesting to apply the methods used by Ramamurty et al to analyze snow. Taking the compaction into account may minimize the differences in apparent macromechanical snow strength detected by the different cone tip angles, as a larger included angle should lead to more compaction.

#### **4.6 Conclusions**

This work demonstrates that it is possible to extract apparent mechanical properties from the force vs. distance signal of cone penetration data. The results from different cone geometries give different, repeatable measures of relative snow strength, with smaller cone



diameter and larger cone included angle correlating with higher apparent snow macromechanical strength.

### **Acknowledgements**

The authors gratefully acknowledge the support of this work by the U.S. Army TACOM Life Cycle Command under Contract No. W56HZV-08-C-0236, through a subcontract with Mississippi State University. This work was performed in part for the Simulation Based Reliability and Safety (SimBRS) research program. Any opinions, findings and conclusions or recommendations expressed in this material are those of the authors and do not necessarily reflect the views of the U.S. Army TACOM.

Disclaimer: Reference herein to any specific commercial company, product, process, or service by trade name, trademark, manufacturer, or otherwise, does not necessarily constitute or imply its endorsement, recommendation, or favoring by the United States Government or the Department of the Army (DoA). The opinions of the authors expressed herein do not necessarily state or reflect those of the United States government or the DoA, and shall not be used for advertising or product endorsement purposes.

## References

- Dowd, T. and R. L. Brown (1986). "A New Instrument for Determining Strength Profiles in Snow Cover." *Journal of Glaciology*, **32**(III): 299-301.
- Fierz, C., R. L. Armstrong, et al. (2009). "The International classification for seasonal snow on the ground." *Technical documents in Hydrology*, **83**: 90 p.
- Haefeli, R. (1939). Snow mechanics: with references to soil mechanics, Translation 14. *Snow and its metamorphism, Snow, Ice and Permafrost Research Establishment*: 57-218.
- Huang, D. and J. H. Lee (2010). "A Method of Using Small-Scale Indentation Tests to Examine Snow Response to Load." *Proceedings of the Joint 9th Asia-Pacific ISTVS Conference and Annual Meeting of Japanese Society for Terramechanics*, Sapporo, Japan.
- Huang, D. and J. H. Lee (2011). A Method of Using A Snow Micro Penetrometer to Obtain Mechanical Properties of Snow. *Joint 17th ISTVS International Conference*. Blacksburg, VA.
- Huang, D. and J. H. Lee (2013). "Mechanical Properties of Snow using Indentation Tests: Size Effects." *Journal of Glaciology*, **59**(213).
- Johnson, J. B. (2000). Characterizing Granular Material Coarseness and Micromechanical Properties using a Small Diameter Penetrometer. *Transportation Research Record, No. 1714*, Transportation Research Board: 83-88.
- Johnson, J. B. (2003). A Statistical Micromechanical Theory of Cone Penetration in Granular Materials, Cold Regions Research and Engineering Laboratory.

- Johnson, J. B. and M. Schneebeli (1999). "Characterizing the microstructural and micromechanical properties of snow." *Cold Regions Science and Technology*, **30**(1-3): 91-100.
- Kirchner, H. O. K., G. Michot, et al. (2001). "Snow as a foam of ice: Plasticity, fracture and the brittle-to-ductile transition" *Philosophical Magazine A*, **81**(9): 2161 - 2181
- LeBaron, A. M., D. A. Miller, et al. (2012). Axisymmetric Measurements of Extended Deformation Around the Snow Micropenetrometer Tip. *International Snow Science Workshop*, Anchorage, Alaska, U.S.A.
- Lee, J. H., D. Huang, et al. (2011). "Statistical Experimental Studies of a Vehicle Interacting with Natural Snowy Terrain for Combined Longitudinal and Lateral Slip." *Proceedings of the 17th International Conference of the International Society of Terrain Vehicle Systems*, Blacksburg, Virginia, United States.
- Mackenzie, R. and W. Payten (2002). A Portable, Variable-Speed, Penetrometer for Snow Pit Evaluation. *International Snow Science Workshop*. Penticton, B.C. Canada.
- Marshall, H. P. and J. B. Johnson (2009). "Accurate inversion of high-resolution snow penetrometer signals for microstructural and micromechanical properties. *Journal of Geophysical Research-Earth Surface*, **114**(F4), F04016
- McCallum, A. B., A. Barwise, et al. (2010). CPT in polar snow - equipment and procedures. 2nd *International Symposium on Cone Penetration Testing*. Huntington Beach, California, U.S.A.
- McCallum, A. B., A. Barwise, et al. (2011). Cone Penetration Testing in Polar Snow. *OTC Arctic Technology Conference*. Houston, Texas, U.S.A., Offshore Technology Conference

- Mellor, M. (1974). A Review of Basic Snow Mechanics, U.S. Army Cold Regions Research and Engineering Laboratory.
- Perla, R. I. and J. M. Martinelli (2004). *Avalanche Handbook*, University Press of the Pacific.
- Ramamurty, U. and M. C. Kumaran (2004). "Mechanical property extraction through conical indentation of a closed-cell aluminum foam." *Acta Materialia*, **52**(1): 181-189.
- Schaap, L. H. J. and P. M. B. Föhn (1987). "Cone penetration testing in snow." *Canadian Geotechnical Journal*, **24**: 335-341.
- Schneebeli, M. and J. B. Johnson (1998). "A constant-speed penetrometer for high-resolution snow stratigraphy." *Annals of Glaciology*, **26**: 107-111.
- Schneebeli, M., C. Pielmeier, et al. (1999). "Measuring snow microstructure and hardness using a high resolution penetrometer." *Cold Regions Science and Technology*, **30**(1-3): 101-114.
- Shapiro, L. H., J. B. Johnson, et al. (1997). "Snow mechanics: review of the state of knowledge and applications." *U.S. Army Cold Regions Research and Engineering Laboratory*. CRREL Report No: CR 97-03(52002236): 35p.
- Yuan, H. (2007). Stochastic reconstruction of snow microstructure from x-ray microtomography images, University of Alaska Fairbanks.

## 5 Discussion and limitations

These three sets of tests have each generated a data set. Although the scatter in the data is high as compared to scatter in mechanical testing of engineered materials, that is to be expected for a natural, granular material whose properties are not controlled by humans. The large variations in natural material properties will always be difficult to account for. Also, this study has deliberately isolated the snow in order to keep it as pure and simple as possible. In application, the properties of the interfacing material will also need to be analyzed and added into the model. In warmer temperatures, the effects of the presence of liquid water menisci will also need to be taken into account. The snow properties and compaction will be greatly affected.

Another factor that was not accounted for in this testing is that the coarse-grained snow type, depth hoar, is known to be highly anisotropic. These three sets of testing were performed in the direction of gravity on the snow samples. However, as friction and plowing tests are pursued, the anisotropic nature of snow will need to be taken into account, particularly with the depth hoar.

Finally, this series of tests has concerned itself only with deep snow (i.e., the bottom is not detected). However, as the snow depth decreases and Zone III from the indentation model (Fig. 2) is approached, the properties of the surface underneath the snow will need to be taken into account. Furthermore, some hardening also occurs during Zone II (as shown by the slight positive slope of Zone II in Fig. 2). This hardening cannot be infinite; deeper snow will need to be tested to verify the extent of hardening that will occur.

## 6 Conclusions

The overarching conclusion of the preceding three chapters is that snow is a geotechnical material and may be tested and analyzed as such. The results sometimes reflect understanding of snow behavior from the standpoint of theory and physics, and other times the results may be purely empirical in nature. However, in both cases, results are repeatable and useable. Snow may in some cases be treated best as an open-celled foam, and in others it may be treated best as a loosely-bonded granular material.

From performing indentation tests, it can be seen that at some finite pin diameter, the size effects disappear as the ratio of indenter size to snow average grain size becomes so high that the snow may be regarded as a continuum. This is the point at which the indentation test becomes essentially an unconfined compression test. This occurs when the pin is about 30 mm in diameter, and this effect is shown in Fig. 21.

Also from the indentation tests, it may be concluded that size effects are exponential in nature. The first peak strength decreased with indenter area according to a power law with an average exponent of 0.84. Furthermore, plateau strength also decreased with increasing indenter area, and snow compaction strength may be calculated from these relationships. For three sets of test data, the compaction strength ranged from 3 to 3.8 kPa, while for a fourth, the compaction strength was 13 kPa. However, large variations in mechanical behavior can reasonably be expected for a natural material. On the whole, exponents correlating with size effects had much better reliabilities than direct strength values from individual tests.

The compression tests yielded plateau strengths that showed that as the indenter size in indentation tests increased, the post-first-peak behavior approached that of an infinite plane.

Other relationships found from unconfined compression testing were that first peak strength, plateau strength, and energy density had no discernible relationship with snow plug volume, surface area, cross-sectional area, cross-sectional diameter, or height. However, they all increased linearly and monotonically with increasing aspect ratio.

The cone penetration tests showed that values for snow micromechanical and macromechanical strength may both be obtained from cone penetration testing.

The original goal of this study was to provide output that could be used as input to more rigorous models for snow. Although many more data sets will need to be obtained to increase confidence, it was demonstrated here that size effects are nontrivial at the mesoscale, and that any model of snow interacting with an interface whose geometry has length scales on the order of mm to cm will need to take the size effects into account. This knowledge should be helpful not only to designers of tires and ground vehicles but to designers of skis, sleds, and other sliding equipment as well.

The suggestion of this study is that when an object that interacts with snow is modeled, the assumed strength of snow used in the design should correspond with the strength on the size scale of the object. For example, if the object is a tire, the tire tread should be used for the characteristic length scale.

Some suggested future work would be to conduct further analysis of the cone penetration data, repeat the testing at higher temperatures to obtain properties of wet snow, and, finally, to conduct testing that combines indentation with sliding, for a more complete analogy of a snow-tire interaction.

## 7 Additional publications by the author

### Journal Papers:

Lee, J.H., D. Huang 2001. Sensitivity analysis, calibration and validation of a snow indentation model. *Journal of Terramechanics*, **49**, pp. 315-32.

Lee, J.H., D. Huang, T. H. Johnson, S. Meurer, A. A. Reid, B. R. Meldrum 2012. Slip-based experimental studies of a vehicle interacting with natural snowy terrain. *Journal of Terramechanics*, **49**, pp. 233-244

### Conference Papers:

Huang, D., J. H. Lee 2011. A method of using a snow micro penetrometer to obtain mechanical properties of snow. *Proceedings of the 17<sup>th</sup> International Conference of the ISTVS*, Blacksburg, VA, USA.

Lee, J.H., D. Huang, T. Johnson 2011. Statistical experimental studies of a vehicle interacting with natural snowy terrain for combined longitudinal and lateral slip. *Proceedings of the 17<sup>th</sup> International Conference of the ISTVS*, Blacksburg, VA, USA.

Huang, D., J. H. Lee 2010. A method of using small-scale indentation tests to examine snow response to load. *Proceedings of the Joint 9<sup>th</sup> Asia-Pacific ISTVS Conference and the Annual Meeting of Japanese Society for Terramechanics*, Sapporo, Japan.

Lee, J.H., D. Huang, T. H. Johnson, S. Meurer, A. A. Reid, B. R. Meldrum 2010. Statistical and slip-based experimental data from vehicle interacting with natural snowy terrain. *Proceedings of the Joint 9th Asia-Pacific ISTVS Conference and the Annual Meeting of the Japanese Society for Terramechanics*, Sapporo, Japan.



- Lee, J.H., T. Johnson, D. Huang, S. Meurer, A. Reid, B. Meldrum 2010. New integrated testing system for the validation of vehicle-snow interaction models. *Proceedings of the 2010 Ground Vehicle Systems Engineering and Technology Symposium (GVSETS), Modeling and Simulation, Testing and Validation (MSTV) Mini-Symposium*, Dearborn, Michigan.
- Lee, J.H., D. Huang 2010. Material point method modeling of porous semi-brittle materials. IOP Conference Series: Materials Science and Engineering, *World Congress of Computational Mechanics*, Sydney, Australia.
- Lee, J.H., D. Huang 2009. A mesoscopic model of low-density snow under rapid loading. Paper number C33A-0484, *American Geophysical Union Annual Conference*, San Francisco, CA.
- Lee, J.H., D. Huang, H.-P. Marshall, J. Johnson 2009. Microscale direct simulation of snow penetration tests and inversion of signals. *11<sup>th</sup> European Regional Conference of the International Society for Vehicle-Terrain Systems*, Bremen, Germany.
- Lee, J.H., D. Huang 2009. Traction on snow and microstructure. *MOCA-09*, Montreal, Quebec, Canada.